Subtilase-mediated biogenesis of the expanded family of SERINE RICH ENDOGENOUS PEPTIDES

Huanjie Yang, Xeniya Kim, Jan Sklenar, Sébastien Aubourg, Gloria Sancho-Andrés, Elia Stahl, Marie-Charlotte Guillou, Nora Gigli-Bisceglia, Loup Tran van Canh, Kyle W Bender, et al.

Subtilase-mediated biogenesis of the expanded family of SERINE RICH ENDOGENOUS PEPTIDES

Huanjie Yang[1,8], Xeniya Kim[1], Jan Sklenar[2], Sébastien Aubourg[3], Gloria Sancho Andrés[4], Elia Stahl[5], Marie-Charlotte Guillou[3], Nora Gigli-Bisceglia[6,9], Loup Tran Van Canh[3], Kyle W. Bender[1], Annick Stintzi[7], Philippe Reymond[5], Clara Sanchez Rodriguez[4], Christa Testerink[6], Jean-Pierre Renou[3], Frank L. H. Menke[2], Andreas Schaller[7], Jack Rhodes[2*], Cyril Zipfel[1,2*]

[1]*Institute of Plant and Microbial Biology, Zurich-Basel Plant Science Center, University of Zurich, Zurich, Switzerland.*

[2]*The Sainsbury Laboratory, University of East Anglia, Norwich Research Park, Norwich, United Kingdom.*

[3]*Université Angers, Institut Agro, INRAE, IRHS, SFR QUASAV, Angers, France.*

[4]*Institute of Molecular Plant Biology, ETH Zurich, Zurich, Switzerland.*

[5]*Department of Plant Molecular Biology, University of Lausanne, Lausanne, Switzerland.*

[6]*Laboratory of Plant Physiology, Wageningen University and Research, Wageningen, 6708 PB, the Netherlands.*

[7]*Institute of Biology, Plant Physiology and Biochemistry, University of Hohenheim, Stuttgart, Germany.*

[8]*Current address: Institute of Genetics and Developmental Biology, Chinese Academy of Sciences, 100101, Beijing, China.*

[9]*Current address: Plant Stress Resilience, Institute of Environmental Biology, Utrecht University, Utrecht, the Netherlands*

[*]Correspondence: Jack Rhodes, jack.rhodes@tsl.ac.uk; Cyril Zipfel, cyril.zipfel@botinst.uzh.ch

Abstract

Plant signalling peptides are typically released from larger precursors by proteolytic cleavage to regulate plant growth, development, and stress responses. Recent studies reported the characterization of a divergent family of *Brassicaceae*-specific peptides,

SERINE RICH ENDOGENOUS PEPTIDES (SCOOPs), and their perception by the leucine-rich repeat receptor kinase MALE DISCOVERER 1-INTERACTING RECEPTOR-LIKE KINASE 2 (MIK2). Here, we reveal that the SCOOP family is highly expanded, containing at least 50 members in the Columbia-0 reference *Arabidopsis thaliana* genome. Notably, perception of these peptides is strictly MIK2-dependent. How bioactive SCOOP peptides are produced, and to which extent their perception is responsible for the multiple physiological roles associated with MIK2 is currently unclear. Using N-terminomics, we validate the N-terminal cleavage site of representative PROSCOOPs. The cleavage sites are determined by conserved motifs upstream of the minimal SCOOP bioactive epitope. We identified subtilases necessary and sufficient to process PROSCOOP peptides at conserved cleavage motifs. Mutation of these subtilases, or their recognition motifs, suppressed PROSCOOP cleavage and associated overexpression phenotypes. Furthermore, we show that higher-order mutants of these subtilases show phenotypes reminiscent of *mik2-1*, consistent with impaired PROSCOOP biogenesis, and demonstrating biological relevance of SCOOP perception by MIK2. Together, this work provides insights into the molecular mechanisms underlying the functions of the recently identified SCOOP peptides and their receptor MIK2.

Introduction

A growing number of plant signalling peptides are being identified and found to play major roles during growth, development and stress responses[1-3]. Such peptides are generally derived from protein precursors; however, relatively few biogenesis mechanisms have been described[2,4-9]. Some plant signalling peptides act as phytocytokines, which are secreted cell-to-cell mobile signals that regulate plant immune responses, analogous to cytokines in metazoans[10-12]. SERINE RICH ENDOGENOUS PEPTIDES (SCOOPs) have recently been reported as a family of phytocytokines transcriptionally induced during stress, especially during biotic interactions[13-15]. SCOOPs are serine-rich, are derived from the C-terminus of divergent secreted PROSCOOPs, and are characterised by the presence of a 13-15 amino acid conserved epitope that includes an 'SxS' motif which is essential for bioactivity[13-15]. PROSOCOOPs undergo maturation steps to produce bioactive SCOOPs[14,16]. Cleavage of PROSCOOP12 was reported to be after R43[14]. For PROSCOOP10, two distinct cleaved peptides (SCOOP10#1 and SCOOP10#2) with hydroxylated prolines

were identified from leaf apoplastic fluids[16]. The exact length of cleaved SCOOPs produced *in planta* and the proteases involved are however unknown. Also, given that synthetic unmodified 13- or 15-mer SCOOP peptides are bioactive[13-15,17], the exact role of potential posttranslational modifications of SCOOPs *in planta* is still unclear. While initially reported as a 14-member family in the genome of the Col-0 ecotype of *Arabidopsis thaliana* (later referred to as *Arabidopsis*)[13], the SCOOP family has recently been shown to contain up to 28 members[14,17]. Active SCOOP peptides induce cellular outputs typical of pattern-triggered immunity such as the production of apoplastic reactive oxygen species (ROS), rapid increase in cytosolic Ca^{2+} concentration, and immune gene expression[13-15,17]. Amongst SCOOPs, SCOOP12 – the founding member of the family – has been studied in more depth and was shown genetically to regulate immunity to diverse pathogens and pests, as well as root growth and ROS homeostasis[13,18,19]. SCOOPs are perceived by the *Arabidopsis* leucine-rich repeat receptor kinase MALE DISCOVERER 1-INTERACTING RECEPTOR LIKE KINASE 2 (MIK2) and recruit the BRASSINOSTEROID INSENSITIVE 1-ASSOCIATED KINASE 1(BAK1) as co-receptor[14,15]. Interestingly, MIK2 is involved in multiple diverse aspects of plant biology, such as responses to the cellulose biosynthesis inhibitor isoxaben (ISX), root growth angle, salt stress tolerance, resistance to the root vascular fungal pathogen *Fusarium oxysporum* 5176 and the generalist herbivore *Spodoptera littoralis*, as well as responsiveness to immune elicitors[14,15,19-23]. Although MIK2 is the sole SCOOP receptor, to which extent the multiple functions of MIK2 are all depending on SCOOP perception is still unknown.

Like most signalling peptides, SCOOPs undergo proteolytic processing to generate an active mature peptide *in planta*; however, little is known mechanistically about this process[14,15]. Many signalling peptides are cleaved by the subtilisin-like serine proteinases, which have been shown to cleave signalling peptides in a sequence- and modification-specific manner to generate bioactive peptides[24,25].

Here we report a comprehensive annotation of putative *PROSCOOP* genes in the *Arabidopsis* Col-0 genome revealing the existence of 50 putative SCOOP peptides, of which at least 36 exhibited MIK2-dependent biological activity, making the SCOOPs one of the largest families of signalling peptides identified in flowering plants. Based upon co-expression during biotic stress, we identify several proteases from subtilase subgroup 3 transcriptionally responsive to the same environmental stimuli as *MIK2*, including biotic elicitor treatment, which promote PROSCOOP cleavage and are

required for PROSCOOP activity *in planta*. Finally, we show that higher order subtilase mutants phenocopy *mik2* mutants suggesting impaired SCOOP signalling.

Results and discussion

Identification of *PROSCOOP* genes within the *A. thaliana* Col-0 genome

Originally, 14 *PROSCOOP* genes were identified in the *Arabidopsis* Col-0 genome[13]. Recently, tolerating more divergence in the core motif, this number was expanded to 23, and then 28 genes[14,17], highlighting the need for a revised bioinformatic analysis of the PROSCOOP family. We comprehensively re-evaluated the PROSCOOP repertoire through iterative searches using BLASTP/TBLASTN and the MOTIF ALIGNMNET AND SEARCH TOOL (part of the MEME suite)[26]. Using this approach, we identified 22 additional putative PROSCOOPs, which we named PROSCOOP29-PROSCOOP50 according to their location within the genome (Extended Data Fig. 1; Extended Data Tables 1 and 2). Despite having low amino acid sequence similarity, all predicted SCOOP peptides have the conserved 'SxS' motif (Extended Data Fig.1) previously shown to be required for activity[13-15]. Interestingly, all of the 30 *PROSCOOP* transcripts detected in our recent RNA-Seq dataset[27] are up-regulated upon elicitor treatment (Extended Data Fig. 2), consistent with their possible function as phytocytokines. Interestingly, some SCOOPs correspond to previously annotated peptides, such as SECRETED TRANSMEMBRANE PEPTIDES (STMPs)[14,15,28], ENHANCER OF VASCULAR WILT RESISTANCE 1 (EWR1)[17,29] and ARACINs[30] (Extended Data Table 2). Notably, some of these peptides were previously shown to have direct antimicrobial activity[28,30], suggesting that PROSCOOPs are analogous to metazoan host-defence peptides (HDPs) encoding dual activities as both immunomodulatory phytocytokines and anti-microbial peptides (AMPs)[31].

To test whether the newly identified SCOOPs are bioactive, we synthesized all of the corresponding 13-mer peptides, and found that many of them induced ROS production and triggered cytosolic Ca^{2+} fluxes when applied exogenously to Col-0 plants (Fig. 1a, b). Importantly, these responses were abolished in *mik2-1* (Extended Data Fig. 3a and b). Notably, while a 13-amino-acid peptide is defined at the minimal active epitope for SCOOP12[13-15], the length of a minimal active epitope appears to vary within the family. For example, the 13-mer derived from SCOOP8 is inactive, but a 15-mer that includes two additional N-terminal amino acids is active (Extended Data Fig. 4a)[14]. Thus, for a selection of inactive 13-mer peptides, we synthesized the corresponding 15-mers and

tested their activity. Several such 15-mer peptides (*e.g.* SCOOP14 and SCOOP40) could induce MIK2-dependent ROS production (Fig. 1c and Extended Data Fig. 3d). In our assays, a few SCOOPs (*e.g.* SCOOP29, SCOOP33, SCOOP35, SCOOP38, SCOOP42, SCOOP48) however remained inactive (either as 13-mer or 15-mer) (Fig. 1 and Extended Data Fig. 5), warranting further investigation of these SCOOPs in the future.

Overall, our data demonstrate that the *Arabidopsis* SCOOP family contains at least 50 members, and that all tested active synthetic SCOOP peptides induce MIK2-dependent responses (Extended Data Fig. 5). In addition, all tested active SCOOPs induce BAK1-dependent ROS production (Extended Data Figure 4b), indicating that SCOOPs induce MIK2-BAK1 complex formation. These findings thus define the SCOOP family as one of the largest families of plant signalling peptides currently known. Strikingly, while other large signalling peptide families, such as CLAVATA3/ENDOSPERM SURROUNDING REGION-RELATED (CLE) peptides, are perceived by several phylogenetically related receptors[32], the perception of all active SCOOP peptides is mediated by a single receptor, MIK2, making this ligand-receptor pair unique within the plant kingdom. Future structural work is required to define the molecular basis of SCOOP binding by MIK2. Some of the synthesized SCOOPs are inactive (Extended Data Fig. 5), possibly because the length and/or posttranslational modifications of peptides are important for activity. Some SCOOPs might also be perceived by another receptor that was lost in Col-0. It is also possible that the SCOOPs could possess other bioactivities, for example direct antimicrobial activity, or they may have become pseudogenized. These are interesting questions to pursue in future work.

PROSCOOP12 is cleaved by SBT3.5

Whilst PROSCOOPs have been shown to undergo proteolytic cleavage[14], the mechanisms by which bioactive SCOOPs are released from PROSCOOPs is still unknown. From the PROSCOOPs sequence alignment (Extended Data Fig. 1), we noticed that most PROSCOOPs contain a 'RxLx/RxxL' motif that is recognized and cleaved by some subtilases (SBTs) including SBT6.1 and SBT3.5[33-37]. Using Genevestigator[38], we observed that among 56 *SBT* genes in *Arabidopsis*[37], *SBT3.3*, *SBT3.4* and *SBT3.5* are transcriptionally up-regulated with *MIK2* under different conditions (Extended Data Fig. 6). These phylogenetically related *SBT* genes were

also amongst the most up-regulated in response to elicitor treatments (Extended Data Fig. 7; Extended Data Fig. 8)[27,39]. Notably, SBT3.3 and SBT3.5 regulate plant immunity and root growth, respectively[37,40], similar to PROSCOOP12[13,19]. Also, the SBT3.5 has a preference for RKLL motif[37], which is similar to a motif found in many PROSCOOP sequences (Extended Data Fig. 1). To test if related SBT3 proteases can cleave PROSCOOPs at such a motif, we focused on PROSCOOP12, the best-characterised PROSCOOP with strong activity[13-15,18,19]. We chose to test cleavage using *Agrobacterium*-mediated transient expression in *Nicotiana benthamiana* which does not contain *SBT3* or PROSCOOP members in its genome[41], thus enabling gain-of-function experiments. As a probe for proteolytic cleavage, we inserted a 6xHA tag between the predicted native signal peptide and PROSCOOP12 coding sequence fused to an in-frame C-terminal GFP tag (SP-6xHA-PROSCOOP12-GFP; Fig. 2a). We then co-expressed this construct with untagged SBT3s (since the presence of a tag could affect SBT protease activity[42-44]). Notably, expression of SBT3.5 resulted in the increased accumulation of a lower molecular weight protein band under flg22 treatment (Fig. 2b and Extended Data Fig. 9a; indicated by a red asterisk) at a size corresponding to SCOOP12-GFP. However, it is not clear whether SBT3.3 and SBT 3.4 could cleave PROSCOOP12 or not in our assays. It could be that SBT3.3 and SBT3.4 cleavage activity is too weak to be detected in this assay. The basal level of the cleaved SCOOP12-GFP products could be caused by endogenous SBTs or other proteases in *Nicotiana benthamiana*.

To test the dependency upon SBT3.5's enzymatic activity, we made use of the specific subtilase inhibitors, EXTRACELLULAR PROTEINASE INHIBITOR 1a and 10 (EPI1a and EPI10), normally produced by the plant pathogen *Phytophthora infestans* as virulence effectors, which have been used previously to assess SBT's functions[4,6,45-48]. As expected, SBT3.5-induced accumulation of the PROSCOOP12 cleavage product was reduced when EPI1a and EPI10 were co-expressed (Fig. 2c). We next sought to establish the importance of the putative subtilase cleavage motif present in PROSCOOP sequences. Mutation of RRLM into AAAA strongly reduced cleavage of PROSCOOP12 by SBT3.5 (Fig. 2d). A previous study showed that PROSCOOP12 is processed at RRLM motif but cleaved downstream of RR[14]. Using mass-spectrometry (MS) coupled with N-terminal labelling (Extended Data Fig. 10), we identified the GSGAGPVR peptide as the N-terminus of the SCOOP12-GFP cleavage product (Extended Data Fig. 11), suggesting the cleavage site is after the RRLM motif *in planta*.

Together, these data indicate SBT3.5 can cleave PROSCOOP12 to release active SCOOP12.

PROSCOOP20 is cleaved by SBT3.6, SBT3.8 and SBT3.9

In addition to PROSCOOPs containing a 'RxLx/RxxL' motif, we noticed a subgroup of PROSCOOPs that lack the 'RxLx/RxxL' motif but contain a 'VWD' motif (Extended Data Fig. 1), a previously reported cleavage motif for the aspartate-dependent subtilase SBT3.8[5,49]. SBT3.6, *SBT3.7*, *SBT3.9* and *SBT3.10* are *SBT3.8* homologues (Extended Data Fig. 8[39]) and *SBT3.7*, *SBT3.9* and *SBT3.10* are highly up-regulated by elicitors treatment (Extended Data Fig. 7). We hypothesized that PROSCOOPs containing the VWD motif could be cleaved by SBT3.8 or its paralogs. To test this, we selected PROSCOOP20, which we recently identified as a 'core immunity response' gene[27]. Using a similar approach, we co-expressed SP-6xHA-PROSCOOP20-GFP (Fig. 3a) with different SBT3s. We found that expression of SBT3.6, SBT3.8 and SBT3.9 led to an increased accumulation of a lower molecular weight protein band, indicative of SCOOP20-GFP (Fig. 3b and Extended Data Fig. 9b; indicated by the red asterisk).

Notably, expression of SBT3.3, 3.4, 3.5 or 3.7 had no apparent effect on PROSCOOP20 cleavage (Fig. 3b), while expression of SBT3.3, 3.4, 3.6, 3.7, 3.8 or 3.9 did not affect PROSCOOP12 cleavage, underlining the specificity of distinct PROSCOOPs cleavage by the different subtilases identified (Fig. 2b). The well-characterised subtilase SBT6.1/S1P did not seem to affect either PROSCOOP12 or PROSCOOP20 cleavage (Fig. 2b and 3b). The ability of the tested SBTs to induce PROSCOOP cleavage thus seems to correlate with the presence of distinct potential cleavage motifs (RRLM for PROSCOOP12, VWD for PROSCOOP20).

The increased accumulation of the cleaved band was reduced by co-expression with the inhibitors EPI1a and EPI10 (Fig. 3c). Similarly, mutation of the predicted 'VWD' motif into 'AAA' reduced PROSCOOP20 cleavage by SBT3.8 (Fig. 3d). These data suggest PROSCOOP20 cleavage is dependent on SBT3.8 activity.

Using N-terminal labelling-coupled MS (Extended Data Fig. 10), DLKIGASGSNSG peptide was detected (Extended Data Fig. 12), while TLLRDLKIGASGSNSG (Extended Data Fig. 13) was only detected once from three replicates, suggesting there could be another cleavage site after VWD motif to produce mature SCOOP20.

We next sought to genetically characterise the role of SBT3.8 in *Arabidopsis.* We were concerned about genetic redundancy as several SBT3.8 paralogs were able to promote PROSCOOP20 cleavage *in planta,* so decided to generate a higher-order *sbt3.6/7/8/9/10* mutant using CRISPR-Cas9[41] (Extended Data Fig. 14). This was facilitated by the tandem genomic arrangement of related SBT3s (Extended Data Fig. 6). Notably, while overexpression of PROSCOOP20 in Col-0 caused a dwarf rosette phenotype, loss of SBT3.6/7/8/9/10 or the processing motif VWD (which was mutated into AAA) suppressed this phenotype (Fig. 3f, e). Together, these data indicate that SBT3.8 and potentially related subtilases mediate the cleavage of PROSCOOP20 around the VWD motif, which is required for SCOOP20-induced signalling.

Loss of *SBT3s* partially phenocopies the loss of *MIK2*

Our study revealed that the SCOOP family is much larger than previously predicted, which renders the genetic characterization of these peptides challenging. As we could demonstrate that different sub-group 3 subtilases are involved in SCOOP cleavage, we generated an octuple mutant for SBT3.3, 3.4, 3.5, 3.6, 3.7, 3.8, 3.9 and 3.10 (*sbt3*^{octuple}) by crossing independent *sbt3.3/4/5* and *sbt3.6/7/8/9/10* mutants generated using CRISPR-Cas9 (Extended Data Fig. 14). The *sbt* higher order mutants didn't show any macroscopic growth and developmental phenotype (Extended Data Fig. 15a), however, the dry weight of *mik2-1* and *sbt*^{octuple} is marginally increased compared with Col-0 (Extended Data Fig 15b). We hypothesised that the *sbt3*^{octuple} mutant is impaired in PROSCOOP processing, and thus provides a genetic background to test for the requirement of SCOOP recognition in different MIK2-dependent processes.

Notably, similar to what observed in *mik2-1*[15], flg22-induced ROS production was impaired in *sbt3*^{octuple} plants (Fig. 4a, b), but not in *sbt3.3/4/5* or *sbt3.6/7/8/9/10* (Extended Data Fig. 15c). MIK2 is also involved in the induction of stress responses upon ISX treatment[21,22]. Induction of the stress marker genes *FRK1* and *CYP81F3* upon ISX treatment was similarly impaired in both *mik2-1* and *sbt3*^{octuple} seedlings (Fig. 4c). Moreover, it was recently demonstrated that MIK2 is required for basal resistance against the generalist herbivore *S. littoralis*[19]. This resistance – as determined by measuring the larvae fresh weight – was also impaired in *sbt3*^{octuple}, albeit to an intermediate level compared to *mik2-1* plants (Fig. 4d).

These data suggest that the control of elicitor-induced ROS production, ISX-induced stress responses and basal resistance to *S. littoralis* all require SBT3 function, and

thus by extension potential PROSCOOP processing and subsequent SCOOP perception by MIK2. However, it must be noted that these subtilases have other targets *in planta* which may contribute to the phenotypes observed. For example, SBT3.8 also cleaves phytosulfokine (PSK) and CLE-LIKE/GOVEN/ROOT GROWTH FACTOR (CLEL/GLV/RGF) peptides, which have reported roles in the regulation of immune signalling[4,49-52]. However, while MIK2 regulates root growth angle[21] and basal resistance to *F. oxysporum*[21,23], *sbt3*^{octuple} plants behaved as wild-type Col-0 plants in these assays (Extended Data Fig. 15d, e), which could be due to non-cleaved PROSCOOPs and the generation of bioactive SCOOPs from some PROSCOOP precursors via subtilases beyond those characterised in our study. Notably, the recent identification of native SCOOP10 peptides in leaf apoplastic fluids suggests that the cleavage of PROSCOOP10, which lacks 'RxLx/RxxL' and 'VWD' motifs, could be dependent upon Y[KR]PN motif reported as cleavage site of subtilases SBT4.12, SBT4.13 and SBT5.2[6,24,25,16]. Furthermore, it is possible that some of the phenotypes observed in the *mik2* mutant may be independent of its function as the SCOOP receptor. Moreover, the strong susceptibility of *mik2* mutant plants to *F. oxysporum* (*Fo*), which is not phenocopied by the loss of SBT3s, suggests that resistance against this fungus may be due to the direct perception of *Fo*-derived elicitors (potentially exhibiting SCOOP-like sequences) by MIK2[14,15,23], which would not necessarily require proteolytic cleavage by a plant subtilase. The exact *Fo*-derived elicitor(s) recognised by MIK2 during infection however remain to be identified.

Collectively, our study provides additional information about the recently identified family of SCOOP peptides, their post-translational processing and biological roles. Notably, as several SCOOPs have been previously proposed as antimicrobial peptides[28,30], it will be interesting to understand the evolutionary and biochemical basis of the dual activity of these SCOOPs. This work also provides a starting point to dissect the multiple functions of MIK2. Notably, it will be interesting in the future to identify which specific SCOOPs mediate these functions, as recently demonstrated for SCOOP12 in the context of herbivory and root growth[18,19].

Acknowledgements

We thank past and present members of the Zipfel laboratory for helpful discussions and comments. Benjamin Brandt and Philipp Köster are particularly thanked for their

assistance with the cloning of the PROSCOOP cleavage constructs. Priya Pimprikar is also thanked for her assistance with the generation of the CRISPR mutants. The authors acknowledge generous funding to study plant immune signalling by the Gatsby Charitable Foundation (CZ), the Biotechnology and Biological Research Council (BB/P012574/1) (CZ), the European Research Council under the European Union's Horizon 2020 research and innovation programme no. 773153 (project 'IMMUNO-PEPTALK') (CZ) and programme no. 72431 (project "Sense2SurviveSalt") (CT), the University of Zurich (CZ), and the Swiss National Science Foundation grants no. 31003A_182625 (CZ) and no. 310030_184769 (CSR).

Author contributions

H.Y., J.R. and C.Z. conceived and designed the experiments. H.Y., J.R., X.K., J.S., S.A., G.S.A., E.S., M.C.G., N.G.B, L.T.V.C. and K.W.B. generated materials, performed experiments, and/or analyzed the data. P.R., C.S.R., A.S., C.T., J.P.R., F.M., A.S., J.R. and C.Z. supervised the project. A.S. contributed conceptually to the study and also provided materials. H.Y., J.R. and C.Z. wrote the manuscript with input from all authors.

Declaration of interests

The authors declare no competing interests.

Figure and Table legends

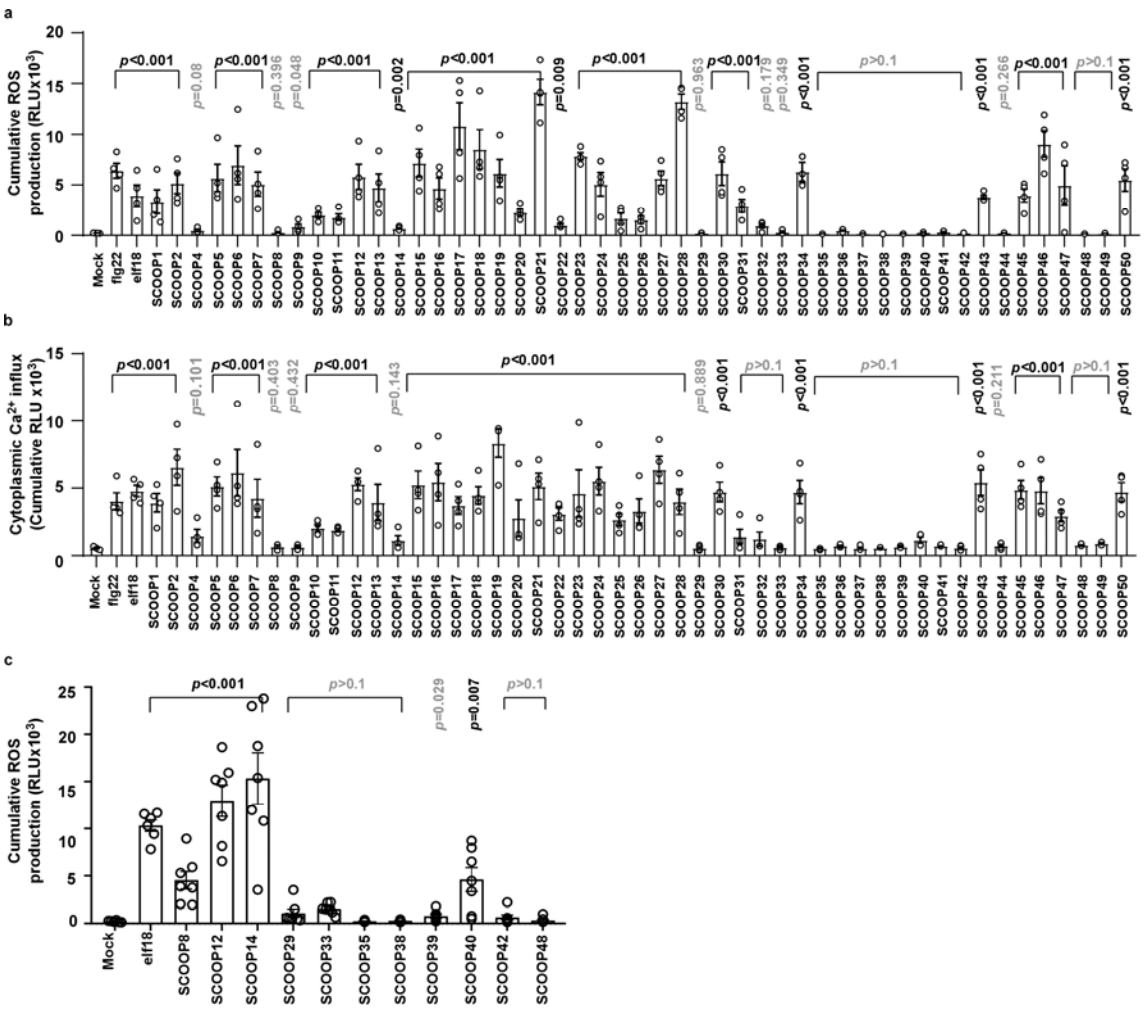

Figure 1 | Divergent SCOOPs induce ROS production and Ca^{2+} influx in Col-0

(a) Integrated ROS production over 40 min in leaf disks collected from 4-week-old plants induced in the absence (Mock) or presence of 1 μM 13-mer SCOOP peptides (n ≥ 8). flg22 and elf18 (100 nM) were used as control to calculate the Z-score to normalise for variation between plates.

(b) Cytoplasmic Ca^{2+} influx measured in Col-0^{AEQ} seedlings induced in the absence (Mock) or presence of 1 μM 13-mer SCOOP peptides (n=4) using 100 nM flg22 and elf18 as control.

(c) Integrated ROS production over 40 min in leaf disks collected from 4-week-old plants induced in the absence (Mock) or presence of 1 μM 15-mer SCOOPs (n ≥ 8) using 100 nM elf18 as control.

Error bars represent SD; P-values indicate significance relative to the mock in a two-tailed T-test. All experiments were repeated and analysed three times with similar results. ROS, reactive oxygen species.

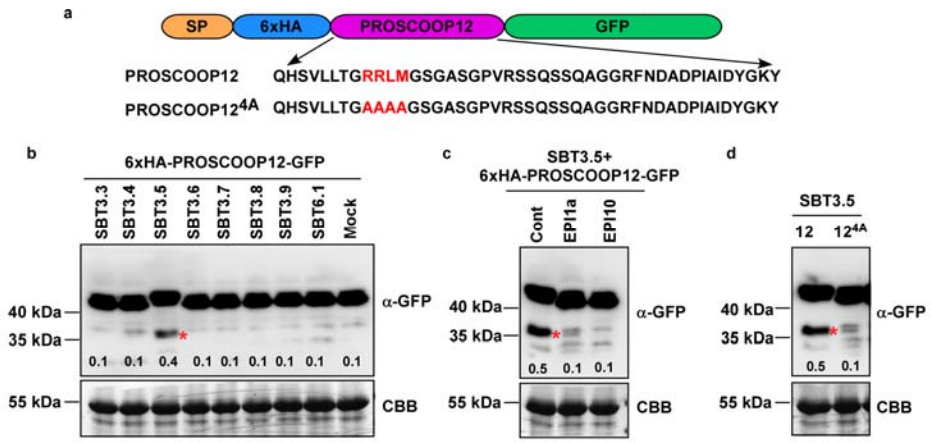

Figure 2 | PROSCOOP12 is cleaved by SBT3.5

(a) Schematic representation of PROSCOOP12 with native signal peptide (SP), N-terminal 6xHA tag and C-terminal GFP tag. The cleavage motif RRLM and mutated residues of RRLM/AAAA are shown as red characters.

(b, c and d) Western blot using GFP antibody recognizing the 6xHA-PROSCOOP12-GFP and truncated SCOOP12-GFP (indicated by the red asterisk) in *Nicotiana benthamiana* leaves after 100 nM flg22 treatment for 2 h. The membrane was stained with CBB, as a loading control. Numbers on the blots correspond to the ratios of protein accumulation levels between truncated proteins bands (indicated by the red asterisk) and full-length protein bands (above the truncated protein bands). (b) Transient co-expression of 6xHA-PROSCOOP12-GFP with SBT3.3, SBT3.4, SBT3.5, SBT3.6, SBT3.7, SBT3.8, SBT3.9, SBT6.1 or without SBT (Mock). (c) Transient co-expression of 6xHA-PROSCOOP12-GFP, SBT3.5 with SBT inhibitors EPI1a/EPI10 or without SBT inhibitor (Mock). (d) Transient co-expression of SBT3.5 with 6xHA-PROSCOOP12-GFP (labelled as 12) or 6xHA-PROSCOOP12^{4A}-GFP (labelled as 12^{4A}). All experiments were repeated and analysed three times with similar results.

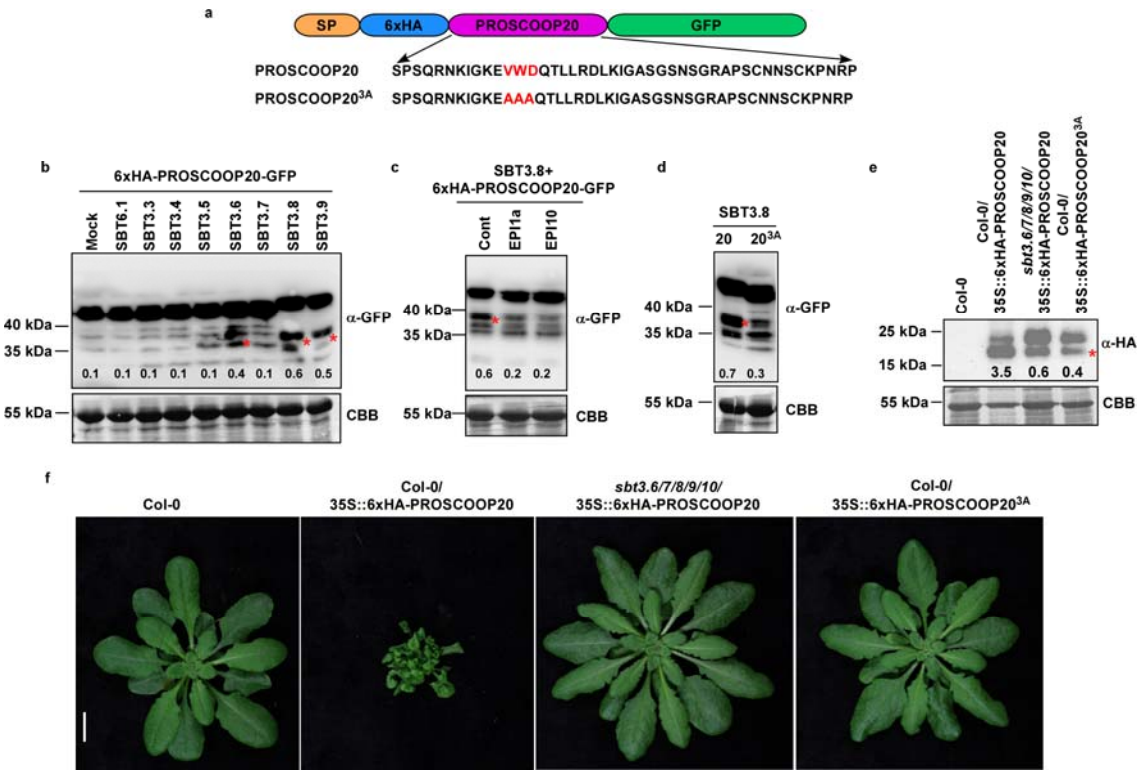

Figure 3 | PROSCOOP20 is cleaved by SBT3.8 and SBT3.9

(a) Schematic representation of PROSCOOP20 with native signal peptide (SP), N-terminal 6xHA tag and C-terminal GFP tag. The cleavage motif VWD and mutated residues of VWD/AAA are shown as red characters.

(b, c and d) Western blot using GFP antibody recognizing the 6xHA-PROSCOOP20-GFP and truncated SCOOP20-GFP (indicated by the red asterisk) in *Nicotiana benthamiana* leaves after 100 nM flg22 treatment for 2 h. The membrane was stained with CBB, as a loading control. Numbers on the blots correspond to the ratios of protein accumulation levels between truncated proteins bands (indicated by the red asterisk) and full-length protein bands (above the truncated proteins bands). (b) Transient co-expression of 6xHA-PROSCOOP20-GFP with or without SBT3.3, SBT3.4, SBT3.5, SBT3.6, SBT3.7, SBT3.8, SBT3.9, SBT6.1 (Mock). (c) Transient co-expression of 6xHA-PROSCOOP-GFP, SBT3.8 with SBT inhibitors EPI1a/EPI10 or without (Mock). (d) Transient co-expression of SBT3.8 with 6xHA-PROSCOOP20-GFP (labelled as 20) or 6xHA-PROSCOOP20^{3A}-GFP (labelled as 20^{3A}). All experiments were repeated and analysed three times with similar results.

(e) Western blot using HA antibody recognizing the 6xHA-PROSCOOP20 in stable transgenic *Arabidopsis* seedings expressing 35S::6xHA-PROSCOOP20 (labelled as 20) or 35S::6xHA-PROSCOOP20^{3A} (labelled as 20^{3A}) in Col-0 or *sbt3.6/7/8/9/10*. The

membrane was stained with CBB, as a loading control. #1: line 1, #2, line 2. Numbers on the blots are the ratios of protein accumulation levels between truncated protein bands (indicated by the red asterisk) and full-length protein bands (above the truncated protein bands).

(f) Phenotype of stable transgenic *Arabidopsis* seedlings expressing 35S::6xHA-PROSCOOP20 or 35S::6xHA-PROSCOOP20^{3A} in Col-0 or *sbt3.6/7/8/9/10.* Bar = 1 cm.

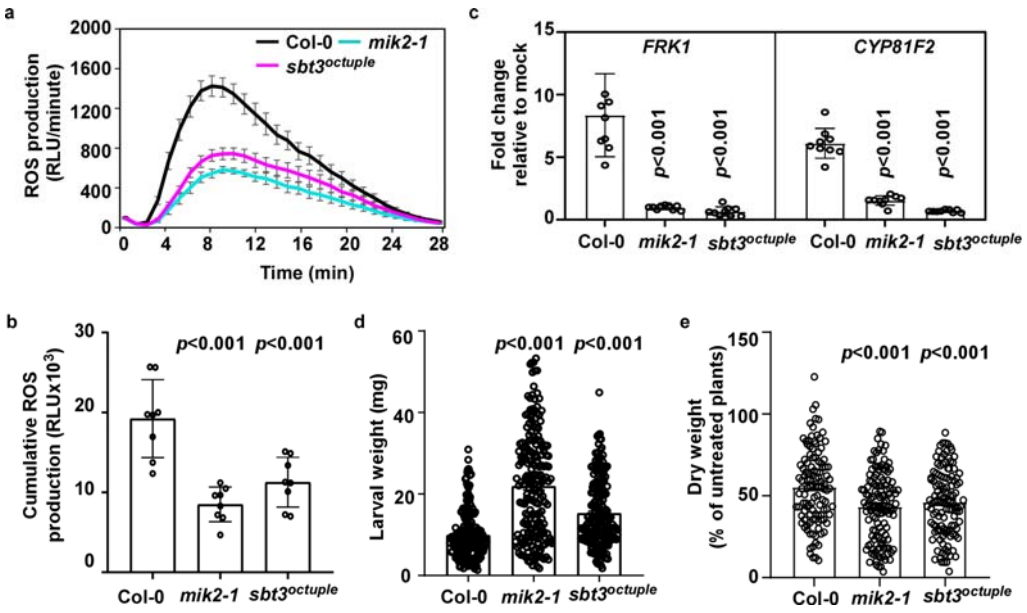

Figure 4 | *sbt3^{octuple}* phenocopies *mik2*

(a and b) ROS production in leaf disks collected from 4-week-old Arabidopsis plants induced by 100 nM flg22 (n = 8). (a) Points represent mean. (b) Integrated ROS production over 30 min.

(c) Immune marker genes expression in 13-day-old *Arabidopsis* seedlings determined by qRT-PCR. Seedlings were treated with 0.6 µM ISX or Mock. Expression of *FRK1* and *CYP81F2* was normalized relative to *Actin7* expression values. Depicted is the fold change in expression relative to mock treatment.

(d) Insect performance of *Spodoptera littoralis* on Col-0, *mik2-1* and *sbt3^{octuple}*. *S. littoralis* larvae were feeding on 5-week-old plants for 12 days. Data represents the mean ± SD of three independent experiments. P-values indicate significance relative to Col-0. (Mann-Whitney-U-Test). Number of individual larvae measured: Col-0 n=215, *mik2-1* n=204 and *sbt3^{octuple}* n=211.

(e) Dry weight of NaCl-treated plants is expressed as percentage of the ratio to the dry weight of untreated plants. One week after germination, plants were transferred to pots with soil saturated with or without 75 mM of NaCl in demineralized water. After 3 weeks of treatment the rosettes were cut, and dry weight was determined.

(a-c, e) Error bars represent SD; P-values indicate significance relative to Col-0 in a two-tailed T-test. All experiments were repeated and analysed three times with similar results.

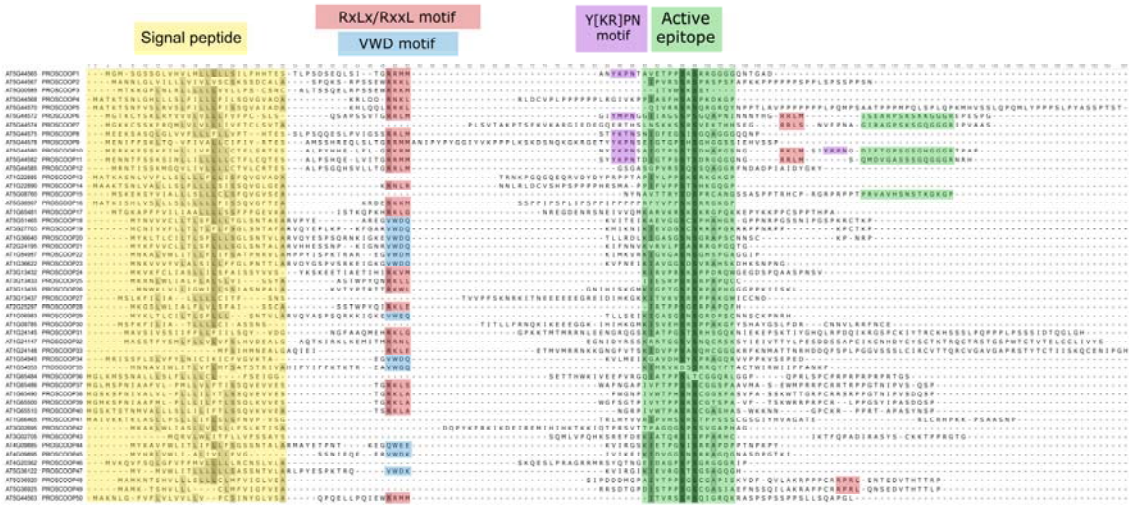

Extended Data Fig. 1 | Sequence alignment of *Arabidopsis* PROSCOOPs

Signal peptide, variable regions containing the predicted cleavage motifs RxLx/RxxL/VWD, and the active epitope containing the conserved motif SxS are indicated by coloured boxes.

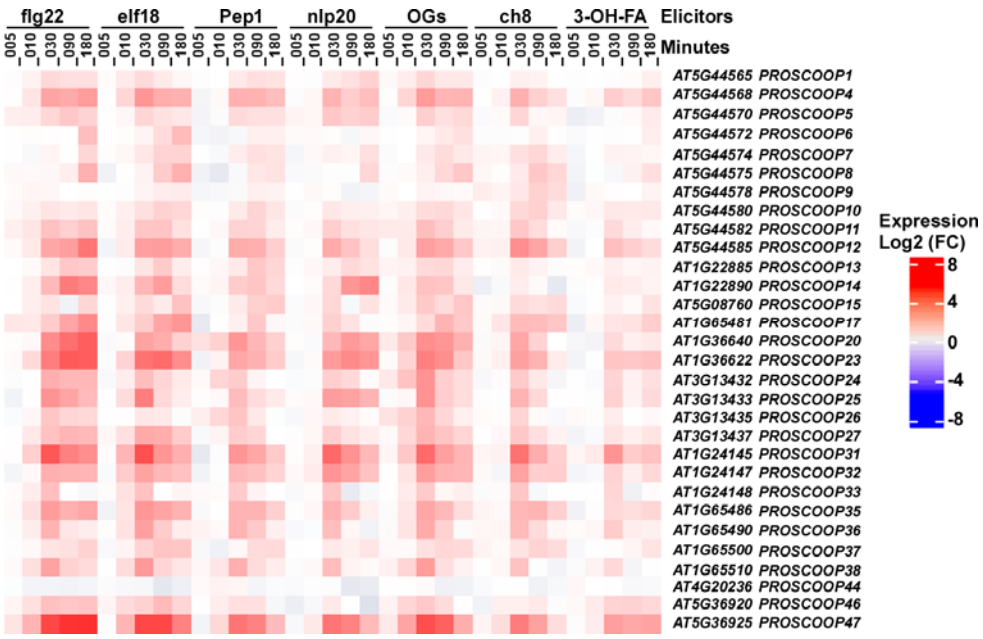

Extended Data Fig. 2 | All *PROSCOOP*s identified by RNA-Seq are up-regulated upon elicitor treatment

Heat map showing $\log_2$(FC) expression levels of *PROSCOOP*s identified by RNA-Seq in response to a range of elicitors (data obtained from[27]).

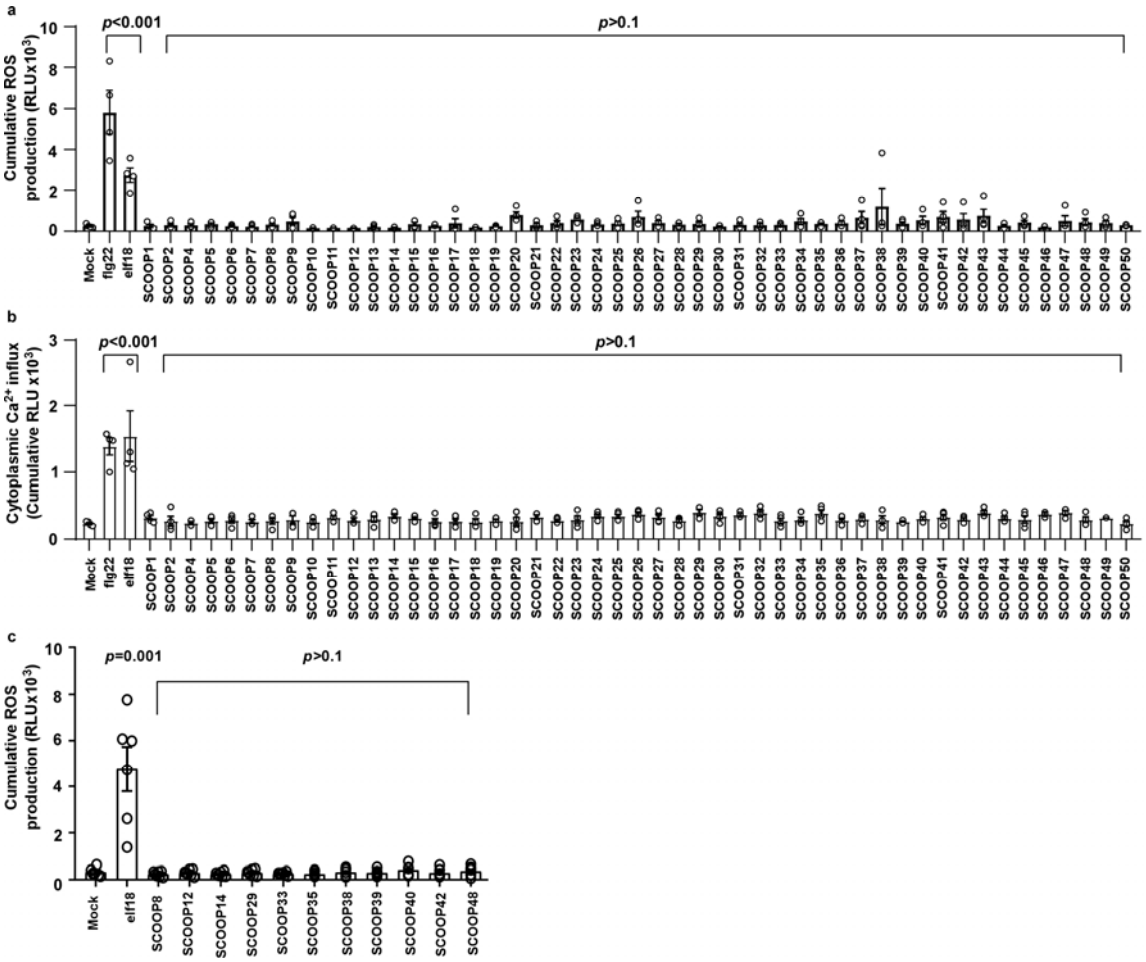

Extended Data Fig. 3 | Divergent SCOOPs do not induce ROS production or Ca^{2+} influx in *mik2-1*

(a) Integrated ROS production over 40 min in leaf disks collected from 4-week-old *Arabidopsis mik2-1* plants induced in the absence (Mock) or presence of 1 μM 13-mer SCOOPs peptides (n ≥ 8) using 100 nM flg22 and elf18 as control.

(b) Cytoplasmic Ca^{2+} influx measured in *mik2-1*^{AEQ} seedlings induced in the absence (Mock) or presence of 1 μM 13-mer SCOOPs peptides (n ≥ 8) using 100 nM flg22 and elf18 as control. (c) Integrated ROS production over 40 min in leaf disks collected from 4-week-old *Arabidopsis mik2-1* plants induced in the absence (Mock) or presence of 15-mer SCOOPs (n ≥ 8) using 100 nM elf18 as control.

Error bars represent SD; P-values indicate significance relative to the mock in a Two-tailed T-test. All experiments were repeated and analysed three times with similar results.

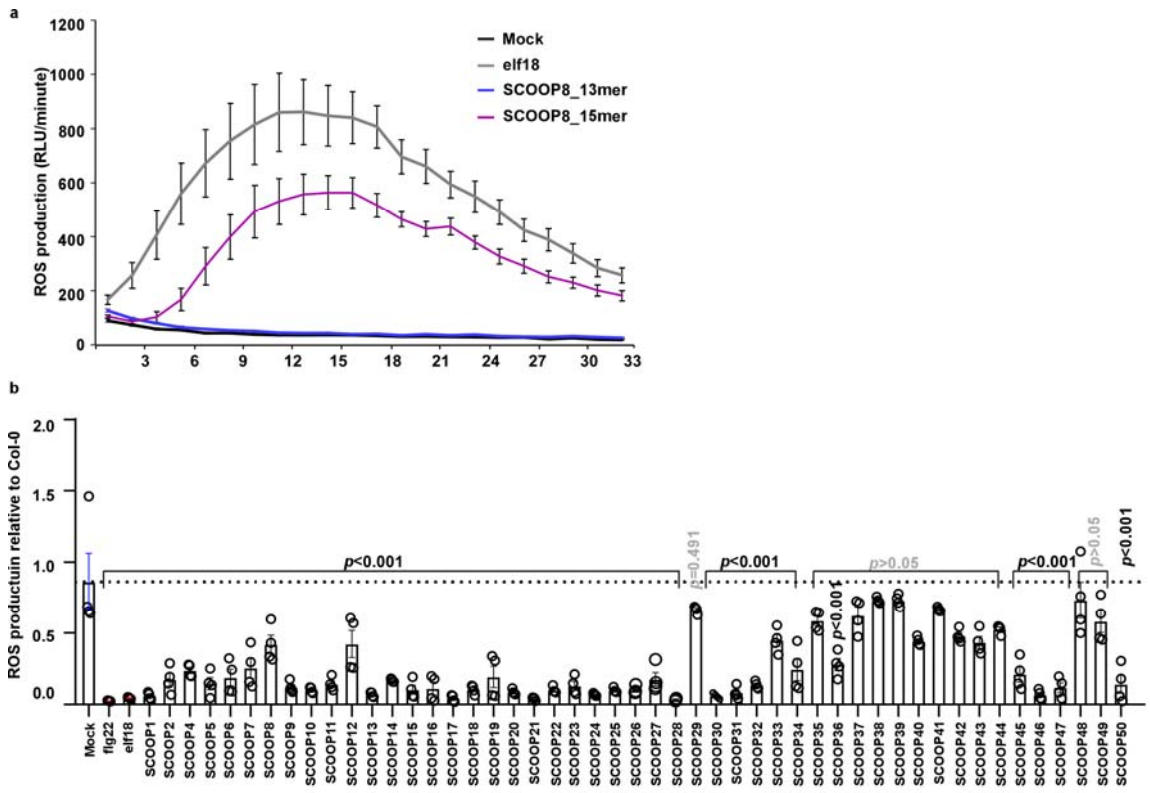

Extended Data Fig. 4 | Additional analysis of SCOOP-induced responses

(a) Integrated ROS production over 40 min in leaf disks collected from 4-week-old *Arabidopsis* plants induced in the absence (Mock) or presence of 1 μM 13/15-mer SCOOP8 peptides (n ≥ 8) using 100 nM elf18 as control.

(b) Integrated ROS production over 40 min in leaf disks collected from 4-week-old *Arabidopsis bak1-5 bkk1* plants relative to Col-0 induced in the absence (Mock) or presence of 1 μM 13-mer SCOOPs peptides (n ≥ 8) using 100 nM flg22 and elf18 as control.

Error bars represent SD; P-values indicate significance relative to the Mock in a Two-tailed T-test. All experiments were repeated and analysed three times with similar results.

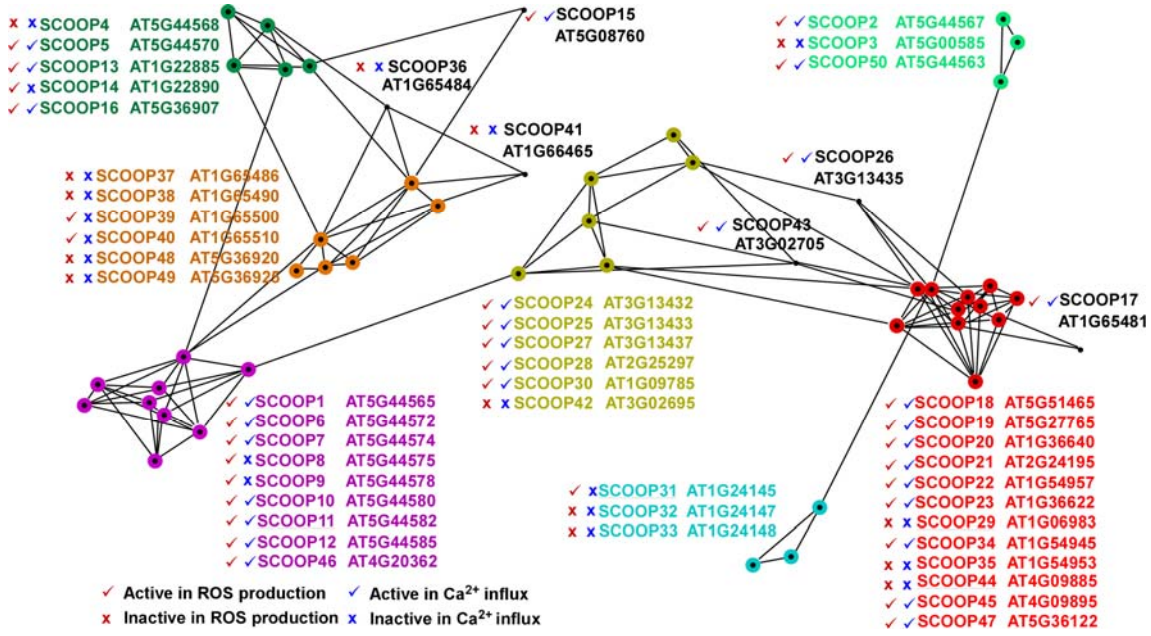

Extended Data Fig. 5 | Similarity relationships inside the PROSCOOP family and summary of SCOOPs activity in Col-0

CLANS clustering based on all-against-all pairwise sequence similarities resulted in 7 groups (highlighted with different colours) and 6 singletons. P-values lower than 1.E-2 and 1.E-5 are represented by grey and black edges respectively.

Coloured asterisk indicates effects of SCOOP peptides.

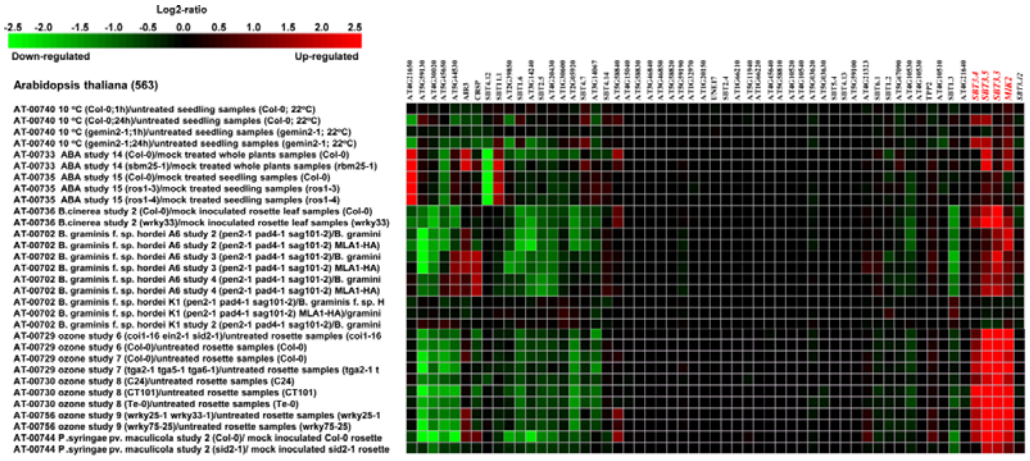

Extended Data Fig. 6 | *SBT3.3/3.4/3.5* are co-regulated with *MIK2* in response to different stresses

Heat map showing log_2(FC) expression levels of *SBT*s in response to stresses (data obtained from Genevestigator).

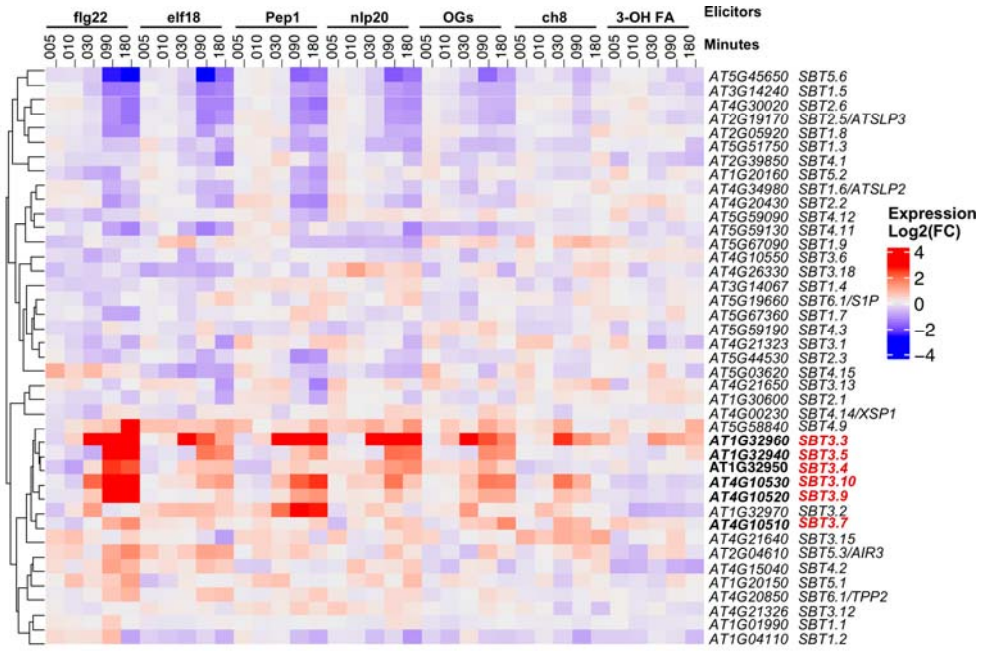

Extended Data Fig. 7 | Transcriptional regulation of Arabidopsis *SBT* genes by elicitors

Heat map showing $\log_2$(FC) expression levels of *SBT* genes in response to a range of elicitors (data obtained from[27]).

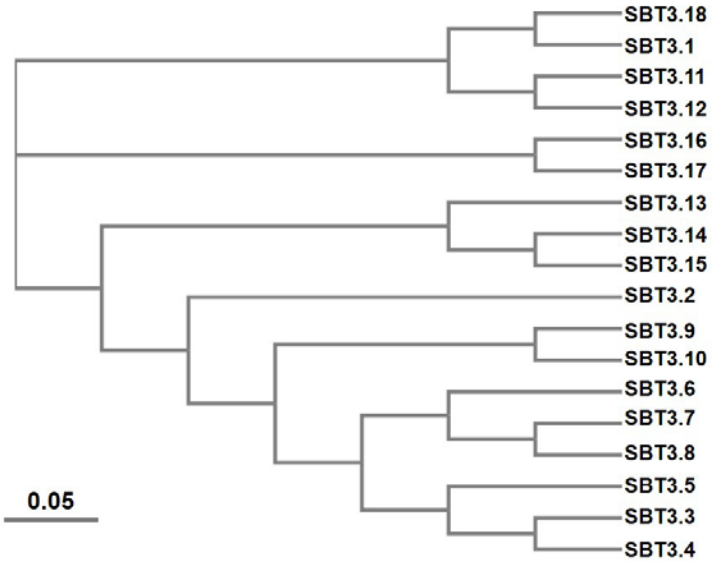

Extended Data Fig. 8 | Phylogeny of Arabidopsis SBT3 subgroup

Phylogeny of the full-length amino acid sequences of SBT3 was inferred using the Maximum-likelihood method and JTT matrix-based model conducted in MEGAX[53].

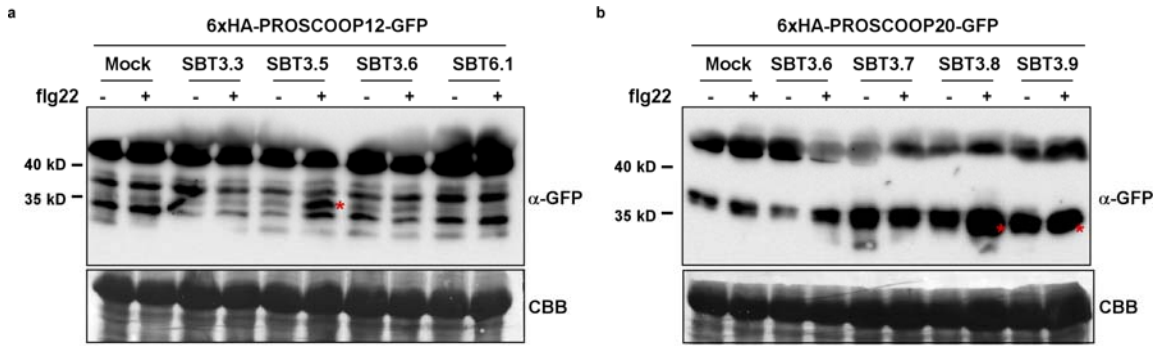

Extended Data Fig. 9| Cleavage analysis of PROSCOOP12 and PROSCOOP20 by different SBTs

(a) Related to Fig. 2 b, indicating flg22-induced SBT3.5-mediated PROSCOOP12 cleavage.

(b) Related to Fig. 3 b, indicating flg22-induced SBT3.6/SBT3.7/SBT3.8-mediated PROSCOOP20 cleavage.

Red asterisks indicate the cleaved SCOOP-GFP bands.

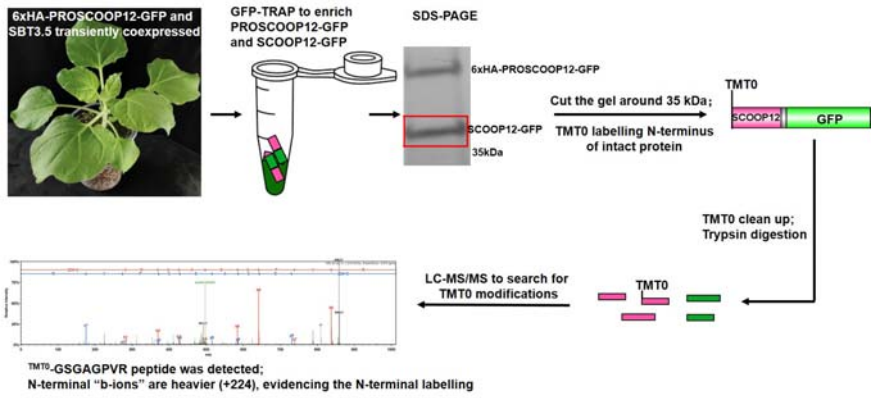

Extended Data Fig. 10| The diagram of TMT-labelling coupled MS

The working flow of TMT-labelling coupled MS to identify SBT3.5-mediated 6xHA-PROSCOOP12-GFP cleavage sites and SBT3.6-mediated 6xHA-PROSCOOP20-GFP cleavage sites in *Nicotiana benthamiana*.

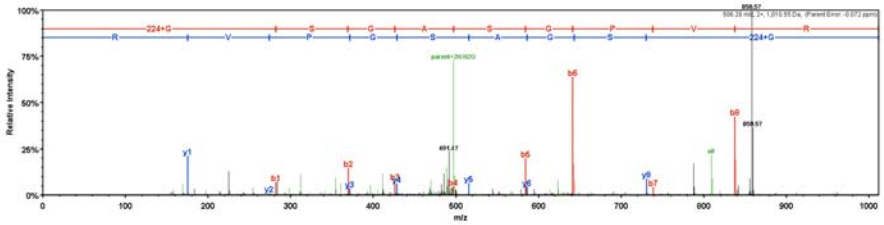

Extended Data Fig. 11 | Mass spectrometry of TMT labelling peptide

TMT-GSGAGPVR peptide was detected by N-terminal labelling-coupled mass spectrometry with three independent experiments.

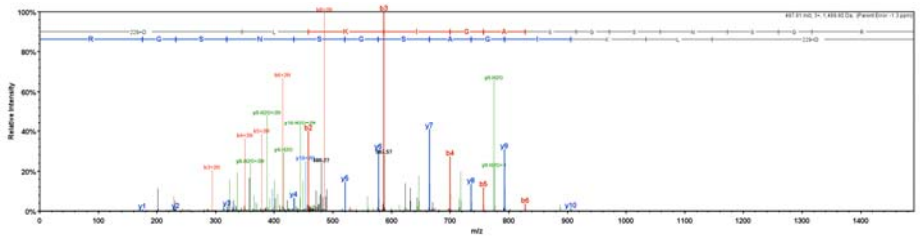

Extended Data Fig. 12 | Mass spectrometry of TMT labelling peptide

TMT-DLKIGASGSNSG peptide was detected by N-terminal labelling-coupled mass spectrometry with three independent experiments.

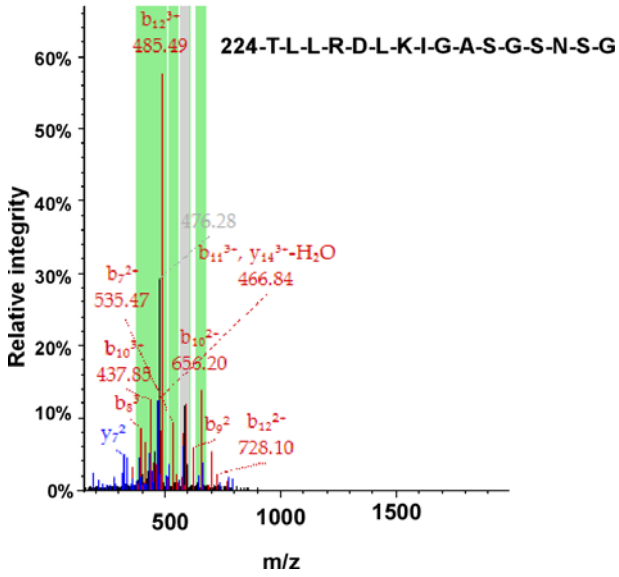

Extended Data Fig. 13 | Mass spectrometry of TMT labelling peptide

TMT-TLLRDLKIGASGSNSG peptide was detected by N-terminal labelling-coupled mass spectrometry with only one time from three repeats.

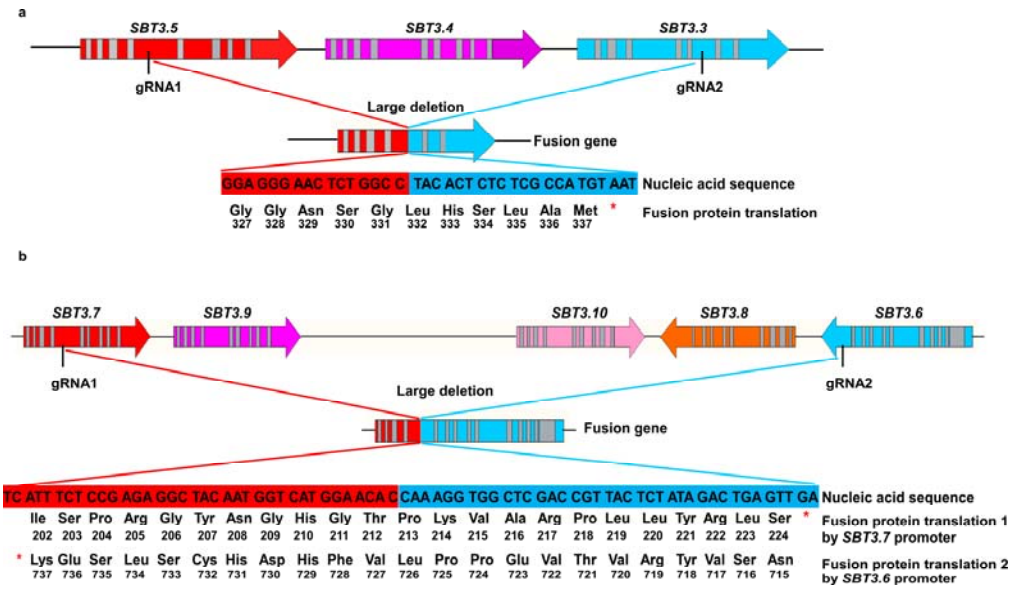

Extended Data Fig. 14 | CRISPR deletes the majority of *SBT3.3/3.4/3.5* and *SBT3.6/3.7/3.8/3.9/3.10* genomic region

(a) Schematic view of the large genomic deletion of clusters *SBT3.3/3.4/3.5*. The fusion protein may be transcribed, consisting of the first 331 amino acids of SBT3.5 with an out-of-frame fusion with SBT3.3 leading to an early stop. Primers F1/R1 and F2/R2 used for the genotyping and sequence (Extended Data Table 3).

(b) Schematic view of the large genomic deletion of clusters *SBT3.6/3.7/3.8/3.9/3.10*. One fusion protein driven by the promoter *SBT3.7* may be transcribed, consisting of 212 amino acid of SBT3.7, fused to 12 nonsense amino acids from SBT3.6 genomic region. Another fusion protein driven by the promoter *SBT3.6* may be transcribed, consisting of 726 amino acids of SBT3.6, fused to 11 nonsense amino acids from SBT3.7 genomic region. Primers F3/R3 and F4/R4 used for the genotyping and sequence (Extended Data Table 3).

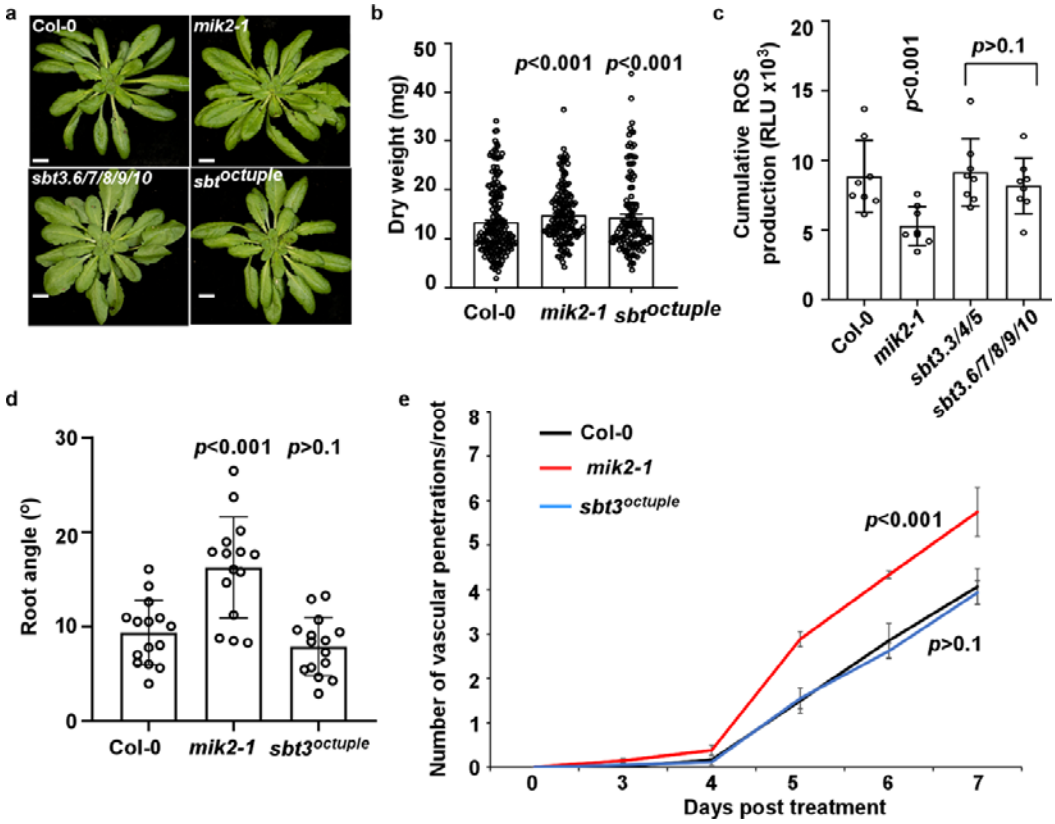

Extended Data Fig. 15 | Phenotypic analysis of *sbt* higher-order mutants

(a) Phenotype of 5-week-old plants. Bar=1cm.

(b) Dry weight of 4-week-old plants. One week after germination, plants were transferred to pots with soil watered from below in demineralized water. After 3 weeks the rosettes were cut, and dry weight was determined.

(c) Integrated ROS production over 30 min in leaf disks collected from 4-week-old Arabidopsis plants induced by 100 nM flg22 application (n=8).

(d) Quantification of the root angle of 9-day-old seedlings grown in an upright position on MS agar medium (n=15).

(e) Cumulative Arabidopsis root vascular penetration by Fo5176 in WT (Col-0), *mik2-1*, and *sbt3*^{octuple} plants at different days post transfer (dpt) to plate-containing spores. Means ± SEM; *N* = 3 replicates, each one containing 20 plants. Statistical significance calculated via repeated measures two-way ANOVA with Tukey post-hoc test (p value ≤ 0.05 (genotype), p value ≤ 0.05 (time), p value ≤ 0.05 (genotype). P values are indicated in the graph with respect to WT at any dpt.

Error bars represent S.D; P-values indicate significance relative to Col-0 in a Two-tailed T-test. All experiments were repeated and analysed three times with similar results.

Material and Methods

Plant material and growth conditions

Arabidopsis thaliana ecotype Columbia (Col-0) was used as wild-type control. Plants for ROS burst assays were grown in individual pots at 21 °C with a 10-h photoperiod. Seeds grown on plates were surface-sterilized using chlorine gas for 5–6 h, and sown on Murashige and Skoog (MS) media supplemented with vitamins, 1 % sucrose, and 0.8 % agar and stratified at 4 °C for 2–3 days. *Nicotiana benthamiana* plants were grown on peat-based media at 24 °C, with 16-h photoperiod.

Aequorin lines of Arabidopsis were described previously[15,54]. *mik2-1* and *sbt3.5-1* mutants have been previously described[21,37].

Synthetic peptides

All synthetic peptides were ordered at >80 % purity (physiological assays) or >95 % purity (biochemical assays) (EZBiolabs). Sequences of all peptides can be found in Supplementary Table 1. The gene models from which the peptide sequences were extracted are listed in Supplementary Table 2.

Molecular cloning

These constructs below were generated by Greengate cloning[55]. pGGZ-35S::SBT3.4 and pGGZ-35S::SBT3.9, pGGZ-35S::6xHA-PROSCOOP12-GFP, pGGZ-35S::6xHA-PROSCOOP12^{4A}(RRLM/AAAA)-GFP, pGGZ-35S::6xHA-PROSCOOP20-GFP, pGGZ-35S::6xHA-PROSCOOP20^{3A}(VWD/AAA)-GFP, pGGZ-35S::6xHA-PROSCOOP20, pGGZ-35S::6xHA-PROSCOOP20^{3A}(VWD/AAA).

The genomic DNA of *SBT3.4* and *SBT3.9* was amplified by PCR. The CDS of 6xHA-PROSCOOP12, 6xHA-PROSCOOP12^{4A} (RRLM/AAAA), 6xHA-PROSCOOP12 and 6xHA-PROSCOOP12^{3A}(VWD/AAAA) were synthesized. Clones were verified by Sanger sequencing.

pGreen0229-pPROSCOOP12::EPI1a/10 was generated by replacing the IDA promoter from the construct pGreen0229-pIDA::EPI1a/10[6]. 1500 bp upstream of the start codon of the PROSCOOP12 gene were amplified by PCR using the primer (Table S3). The PCR products and pGreen0229-pIDA::EPI1a/10 were digested with NotI and PstI. Then the PCR product was cloned into the respective restriction sites of pGreen0229 upstream of the EPI1a or EPI10 constructs.

Expression constructs pART27-35S::SBT3.5 and pART7-35S::SBT3.8 have been described previously[5,37]. Expression constructs for SBT3.3 and SBT3.7 were

generated accordingly. Briefly, the open reading frames of SBT3.3 and SBT3.7 were amplified by PCR and cloned into the multiple cloning site of pART7[56], between the CaMV-35S promoter and terminator. The expression cassette was then transferred into the NotI site of the binary vector pART27[56].

CRISPR-Cas9 mutagenesis

CRISPR-Cas9 induced mutagenesis was performed as described[57]. The *RPS5a* promoter drove Cas9 expression and FASTred selection was used for positive and negative selection. Primers used to generate the vectors can be found in Extended Data Table 3. Mutants were screened by PCR genotyping and confirmed by Sanger sequencing. Primers used for genotyping and sequencing can be found in Extended Data Table 3.

ROS measurement

Leaf disks were harvested from 4-week-old *Arabidopsis* plants using a 4-mm diameter biopsy punch (Integra™ Miltex™) and placed into white 96-well-plates (655075, Greiner Bio-One) containing 100 µL water. Leaf disks were rested overnight. Prior to ROS measurement, the water was removed and replaced with ROS assay solution (100 µM Luminol (123072, Merck), 20 µg mL^{-1} horseradish peroxidase (P6782, Merck)) with or without elicitors. Immediately after light emission was measured from the plate using a HIGH-RESOLUTION PHOTON COUNTING SYSTEM (HRPCS218, Photek) equipped with a 20 mm F1.8 EX DG ASPHERICAL RF WIDE LENS (Sigma Corp). For assays were not all treatments could be conducted on one plate a Z-score was calculated. Internal controls of mock and 100 nM elf18 were included on each plate Z(standard score) = x (integrated ROS production for one leaf disk) - µ (Mean integrated ROS production for mock treatment) / σ (standard deviation of integrated ROS production for mock treatment) as performed previously[58].

Cytoplasmic Ca^{2+} measurement

Seedlings were initially grown on 1/2 MS plated for 3 days before being transferred to 96-well plates (655075, Greiner Bio-One) in 100 µL liquid MS for 5 days. The evening before Ca^{2+} measurements the liquid MS was replaced with 100 µL 20 µM coelenterazine (EC14031, Carbosynth) and the seedlings incubated in the dark overnight. The following morning the coelenterazine solution was replaced with 100 µL water and rested for a minimum of 30 min in the dark. Readings were taken in a VARIOSKAN™ MUTIPLATE READER (ThermoFisher) before and after adding 50 µL

of 3 x concentrated elicitor solution or Mock. Readings were normalised to the average RLU value before elicitor addition (L_0).

CLANs clustering of PROSCOOP family

The 50 PROSCOOP sequences have been analysed and clustered using the CLANS software based on all-against-all BLASTP pairwise sequence similarities[59]. P-value cut-off has been set to 1.E-2 for edge definition and the Convex method (stdev cut-off 0.5, minimum of 3 sequences per cluster) has been applied for clustering.

Transient expression in *Nicotiana benthamiana*

Agrobacterium tumefaciens strain GV3101 transformed with the appropriate construct were grown overnight in L-media and spun-down. The bacteria were resuspended in 10 mM $MgCl_2$ and adjusted to $O.D._{600} = 0.2$ prior to infiltration into the youngest fully expanded leaves of 3-week-old plants. Two days later, leaf tissues were collected, treated in liquid MS medium by 100 nM flg22 for 2 hours and flash-frozen in liquid nitrogen.

Protein extraction and western blot

N. benthamiana leaf tissues were flash-frozen in liquid nitrogen. Plant tissue was ground in liquid nitrogen prior to boiling in 2× loading sample buffer (4 % SDS, 20 % glycerol, 10 % 2-mercaptoethanol, 0.004% bromophenol blue, and 0.125 M Tris-HCl; (10 µL.mg−1 tissue)) for 10 min at 95 °C. The samples were then spun at 13,000 × g for 5 min prior to loading and running on SDS-PAGE gels of an appropriate concentration. Proteins were transferred onto PVDF membrane (ThermoFisher) prior to incubation with appropriate antibodies (α-HA-HRP (12013819001, Roche, 1:3000); α-RFP-HRP (sc-9996 HRP, Santa Cruz, 1:5000) and α-GFP-HRP (A-0545, Merck; 1:50000). Western blots were imaged with a LAS 4000 IMAGEQUANT SYSTEM (GE Healthcare). Staining of the blotted membrane with Coomassie brilliant blue was used to confirm loading.

GFP-TRAP enrichment

After protein extraction from *N. benthamiana* leaf tissues, the 6xHA-PROSCOOP12/20-GFP and SCOOP12/20-GFP was enriched by GFP-TRAP. Proteins were extracted using the extraction buffer (50 mM Tris pH 7.5, 150 mM NaCl, 2.5 mM EDTA, 10 % Glycerol, 1 % IGEPAL, 5 mM DTT, 1 % Plant Protease Inhibitor (P9599, Sigma)) (v/v). Proteins were solubilised at 4 °C with gentle agitation for 30 min before filtering through miracloth. The filtrate was centrifuged at 15000 x g for 20 min at 4 °C. An input sample was taken. To each 15 mL of protein extract 40 µL of GFP-

TRAP AGAROSE BEADS (50 % slurry, ChromoTek) washed in extraction buffer were added and incubated with gentle agitation for 4 h at 4 °C. Beads were harvested by centrifugation at 1500 x g for 2 min and washed 3 times in extraction buffer. 50 µL of 1.5 x elution buffer (NuPage) were added and incubated at 90 °C for 10 min. The samples were then spun at 13,000 × g for 5 min prior to loading and running on SDS-PAGE gels of an appropriate concentration. Samples were then cut from the SDS-PAGE gel for subsequent MS analysis.

N-terminal labelling and mass spectrometry

Proteins separated by SDS-PAGE were excised, destained with 25% Acetonitrile, reduced by 10mM DTT 55 °C for 30min, and carbamidomethylated with 40mM chloroacetamide. The gel was washed with copious exchanges of 50mM TEAB and dehydrated with 100% acetonitrile. Protein free N-termini were labelled with 100µg TMT reagent (ThermoFisher) dissolved in 20µL 100% acetonitrile and directly added to the gel followed by 80 µL of 50mM TEAB (ThermoFisher) buffer. The reaction left at room temperature for 90min was subsequently quenched with 5% hydroxylamine; after this, all proteoforms with accessible N-termini should be N-terminally TMT-labelled.

The reagent leftovers were extracted by 50mM ammonium bicarbonate buffer and the gel dehydrated with 100% acetonitrile. Proteins were in-gel digested by 100ng of trypsin (ThermoFisher), peptides extracted with 25% Acetonitrile, freeze-dried and measured by Orbitrap Eclipse (ThermoFisher Scientific) LC-MS system with a data-dependent acquisition MS method.

The data were processed with a common proteomic pipeline consisting of MS Convert program to generate peak-lists followed by peptide sequence matching on Mascot (Matrix Science Ltd.) server. The individual samples were compared and tandem mass spectra visualized in Scaffold (Proteome Software Inc.).

RNA extraction and qRT-PCR

Two 5-day-old seedlings were transferred into transparent 24-well plates (Greiner Bio-One) containing 1 mL liquid MS media, sealed with porous tape and grown for a further 7 days. The liquid MS media was taken out and 1 mL fresh liquid MS medium containing 600 nM isoxaben (ISX) (Sigma-Aldrich, St. Louis, MO, USA) or Mock was added, and seedlings were harvested after 9 h treatment. All seedlings were ground in liquid nitrogen. Total RNA was extracted using plant total RNA mini kit (FavorPrep) according to the manufacturer’s instructions and DNase treatment was performed using the RNeasy kit (Qiagen). RNA was quantified with a Nanodrop

spectrophotometer (Thermo Fischer Scientific). qRT-PCR was performed on cDNA synthesised using the RevertAid first strand cDNA synthesis kit (Thermo Fisher Scientific) according to the manufacturer's instructions. cDNA was amplified by quantitative PCR using PowerUP SYBR Green Master mix (Thermo Fischer Scientific) running on an Applied Biosystems 7500 Fast Real-Time PCR System (Thermo Fischer Scientific).

Insect performance

Spodoptera littoralis (Egyptian cotton worm) eggs were obtained from Syngenta (Stein AG; Switzerland). For hatching, *S. littoralis* eggs were incubated for 48 h at 28 °C. For measurements of insect performance, 60–80 freshly hatched *S. littoralis* larvae were placed on 11 5-week-old plants per genotype in transparent plexiglass boxes.*S. littoralis* larvae were allowed to feed on those plants for 12 days and individual larval weights were determined subsequently on a high precision balance (Mettler-Toledo; XP205DR, Switzerland).

***Fusarium oxysporum* 5176 infection assay**

Plants were infected on plates as previously described[60,61]. Briefly, seeds were germinated on Whatman filter paper strips in ½ MS+0.9% agar. Eight-day-old seedling were transferred to a mock or infection plate. The infection plates were prepared by spreading 100 µL 1 x 10^7 pSIX1:GFP spores / mL on the MS+0.9% bactoagar surface. Vascular penetration sites were recorded from 3 to 7 days post transfer (dpt) to spore-containing plates, determined when strong and linear signals were visible under a Leica M205 FCA fluorescent stereo microscope equipped with a long pass GFP filter (ET GFP LP; Excitation nm: ET480/40x; Emission nm: ET510 LP).

Root skewing assay

Seeds were sown directly on 1/2 MS agar square plates and stratified for 2 days at 4 °C. Plates were transferred to 22 °C under a 16-h photoperiod, in an upright position for 9 d. The root angle was measured by the ImageJ software, as performed previously[21].

Salt tolerance assays

Salt tolerance assays were performed as previously[21]. Plants were grown in pots under an 11-h photoperiod, at 22 degrees and 70% humidity. One week after germination, plants were transferred to pots which were saturated with 4 L of either 0 or 75 mM of NaCl solution. During the experiment, all plants were watered with demineralized water from below. After 3 weeks of treatment, plants were cut off and dried in an oven at 70

degrees for 1 week to determine dry weight. Plants were randomised over trays using a randomized block design. Randomisation was similar for each treatment. The experiment was repeated three times with similar results

References

1 Matsubayashi, Y. Posttranslationally modified small-peptide signals in plants. *Ann Rev Plant Biol* **65**, 385-413 (2014).

2 Olsson, V. *et al.* Look closely, the beautiful may be small: precursor-derived peptides in plants. *Ann Rev Plant Biol* **70**, 153-186 (2019).

3 Tavormina, P., De Coninck, B., Nikonorova, N., De Smet, I. & Cammue, B. P. The plant peptidome: an expanding repertoire of structural features and biological functions. *Plant cell* **27**, 2095-2118 (2015).

4 Stührwohldt, N., Ehinger, A., Thellmann, K. & Schaller, A. Processing and formation of bioactive CLE40 peptide are controlled by posttranslational proline hydroxylation. *Plant Physiol* **184**, 1573-1584 (2020).

5 Stührwohldt, N. *et al.* The biogenesis of CLEL peptides involves several processing events in consecutive compartments of the secretory pathway. *Elife* **9,** (2020).

6 Schardon, K. *et al.* Precursor processing for plant peptide hormone maturation by subtilisin-like serine proteinases. *Science* **354**, 1594-1597 (2016).

7 Reichardt, S., Piepho, H. P., Stintzi, A. & Schaller, A. Peptide signaling for drought-induced tomato flower drop. *Science* **367**, 1482-1485 (2020).

8 Doll, N. M. *et al.* A two-way molecular dialogue between embryo and endosperm is required for seed development. *Science* **367**, 431-435 (2020).

9 Stührwohldt, N. & Schaller, A. Regulation of plant peptide hormones and growth factors by post-translational modification. *Plant Biol* **21**, 49-63 (2019).

10 Rzemieniewski, J. & Stegmann, M. Regulation of pattern-triggered immunity and growth by phytocytokines. *Curr Opin Plant Biol* **68**, 102230 (2022).

11 Hou, S., Liu, D. & He, P. Phytocytokines function as immunological modulators of plant immunity. *Stress Biol* **1**, 8 (2021).

12 Gust, A. A., Pruitt, R. & Nürnberger, T. Sensing danger: key to activating plant immunity. *Trends Plant Sci* **22**, 779-791 (2017).

13 Gully, K. *et al.* The SCOOP12 peptide regulates defense response and root elongation in Arabidopsis thaliana. *J Exp Bot* **70**, 1349-1365 (2019).

14 Hou, S. *et al.* The Arabidopsis MIK2 receptor elicits immunity by sensing a conserved signature from phytocytokines and microbes. *Nature Commun* **12**, 5494 (2021).

15 Rhodes, J. *et al.* Perception of a divergent family of phytocytokines by the Arabidopsis receptor kinase MIK2. *Nature Commun* **12**, 705 (2021).

16 Guillou, M.-C. *et al.* The PROSCOOP10 gene encodes two extracellular hydroxylated peptides and impacts flowering time in Arabidopsis. *Plants (Basel)* **11**, 3354 (2022).

17 Zhang, J. *et al.* EWR1 as a SCOOP peptide activates MIK2-dependent immunity in Arabidopsis. *J Plant Inter* **17** (2022).

18 Guillou, M. C. *et al.* SCOOP12 peptide acts on ROS homeostasis to modulate cell division and elongation in Arabidopsis primary root. *J Exp Bot* **73**, 6115-6132 (2022).

19 Stahl, E. *et al.* The MIK2/SCOOP signaling system contributes to Arabidopsis resistance against herbivory by modulating jasmonate and Indole glucosinolate biosynthesis. *Front Plant Sci* **13**, 852808 (2022).

20 Julkowska, M. M. *et al.* Natural variation in rosette size under salt stress conditions corresponds to developmental differences between Arabidopsis accessions and allelic variation in the LRR-KISS gene. *J Exp Bot* **67**, 2127-2138 (2016).

21 Van der Does, D. *et al.* The Arabidopsis leucine-rich repeat receptor kinase MIK2/LRR-KISS connects cell wall integrity sensing, root growth and response to abiotic and biotic stresses. *PLoS Genet* **13**, e1006832 (2017).

22 Engelsdorf, T. *et al.* The plant cell wall integrity maintenance and immune signaling systems cooperate to control stress responses in Arabidopsis thaliana. *Sci Signal* **11**, (2018).

23 Coleman, A. D. *et al.* The Arabidopsis leucine-rich repeat receptor-like kinase MIK2 is a crucial component of early immune responses to a fungal-derived elicitor. *New Phytol* **229**, 3453-3466 (2021).

24 Stintzi, A. & Schaller, A. Biogenesis of post-translationally modified peptide signals for plant reproductive development. *Curr Opin Plant Biol* **69**, 102274 (2022).

25 Royek, S. *et al.* Processing of a plant peptide hormone precursor facilitated by posttranslational tyrosine sulfation. *Proc Natl Acad Sci U S A* **119**, e2201195119 (2022).
26 Bailey, T. L. & Gribskov, M. Combining evidence using p-values: application to sequence homology searches. *Bioinformatics* **14**, 48-54 (1998).
27 Bjornson, M., Pimprikar, P., Nürnberger, T. & Zipfel, C. The transcriptional landscape of Arabidopsis thaliana pattern-triggered immunity. *Nat Plants* **7**, 579-586 (2021).
28 Yu, Z. *et al.* The Brassicaceae-specific secreted peptides, STMPs, function in plant growth and pathogen defense. *J Inte Plant Biol* **62**, 403-420, (2020).
29 Yadeta, K. A., Valkenburg, D. J., Hanemian, M., Marco, Y. & Thomma, B. P. The Brassicaceae-specific EWR1 gene provides resistance to vascular wilt pathogens. *PloS One* **9**, e88230 (2014).
30 Neukermans, J. *et al.* ARACINs, Brassicaceae-specific peptides exhibiting antifungal activities against necrotrophic pathogens in Arabidopsis. *Plant Physiol* **167**, 1017-1029 (2015).
31 Petre, B. Toward the discovery of host-defense peptides in plants. *Front Immun* **11**, 1825 (2020).
32 Fletcher, J. C. Recent advances in Arabidopsis CLE peptide signaling. *Trends Plant Sci* **25**, 1005-1016 (2020).
33 Liu, J. X., Srivastava, R., Che, P. & Howell, S. H. Salt stress responses in Arabidopsis utilize a signal transduction pathway related to endoplasmic reticulum stress signaling. *Plant J* **51**, 897-909 (2007).
34 Liu, J. X., Srivastava, R., Che, P. & Howell, S. H. An endoplasmic reticulum stress response in Arabidopsis is mediated by proteolytic processing and nuclear relocation of a membrane-associated transcription factor, bZIP28. *Plant Cell* **19**, 4111-4119 (2007).
35 Ghorbani, S. *et al.* The SBT6.1 subtilase processes the GOLVEN1 peptide controlling cell elongation. *J Exp Bot* **67**, 4877-4887 (2016).
36 Abarca, A., Franck, C. M. & Zipfel, C. Family-wide evaluation of RAPID ALKALINIZATION FACTOR peptides. *Plant Physiol* **187**, 996-1010 (2021).
37 Sénéchal, F. *et al.* Arabidopsis PECTIN METHYLESTERASE17 is co-expressed with and processed by SBT3.5, a subtilisin-like serine protease. *Ann Bot* **114**, 1161-1175 (2014).

804 38 Hruz, T. *et al.* Genevestigator v3: a reference expression database for the meta-
805 analysis of transcriptomes. *Adv Bioinformatics* **2008**, 420747 (2008).
806 39 Schaller, A. *et al.* From structure to function - a family portrait of plant subtilases.
807 *New Phytol* **218**, 901-915 (2018).
808 40 Ramírez, V., López, A., Mauch-Mani, B., Gil, M. J. & Vera, P. An extracellular
809 subtilase switch for immune priming in Arabidopsis. *PLoS Pathog* **9**, e1003445
810 (2013).
811 41 Kourelis, J. *et al.* A homology-guided, genome-based proteome for improved
812 proteomics in the alloploid Nicotiana benthamiana. *BMC Genomics* **20**, 722
813 (2019).
814 42 von Groll, U., Berger, D. & Altmann, T. The subtilisin-like serine protease SDD1
815 mediates cell-to-cell signaling during Arabidopsis stomatal development. *Plant*
816 *Cell* **14**, 1527-1539 (2002).
817 43 Cedzich, A. *et al.* The protease-associated domain and C-terminal extension
818 are required for zymogen processing, sorting within the secretory pathway, and
819 activity of tomato subtilase 3 (SlSBT3). *J Biol Chem* **284**, 14068-14078, (2009).
820 44 Ottmann, C. *et al.* Structural basis for Ca2+-independence and activation by
821 homodimerization of tomato subtilase 3. *Proc Natl Acad Sci U S A* **106**, 17223-
822 17228 (2009).
823 45 Stührwohldt, N., Schardon, K., Stintzi, A. & Schaller, A. A toolbox for the nalysis
824 of peptide signal biogenesis. *Molecular Plant* **10**, 1023-1025 (2017).
825 46 Tian, M., Huitema, E., Da Cunha, L., Torto-Alalibo, T. & Kamoun, S. A Kazal-
826 like extracellular serine protease inhibitor from Phytophthora infestans targets
827 the tomato pathogenesis-related protease P69B. *J Biol Chem* **279**, 26370-
828 26377 (2004).
829 47 Tian, M., Benedetti, B. & Kamoun, S. A Second Kazal-like protease inhibitor
830 from Phytophthora infestans inhibits and interacts with the apoplastic
831 pathogenesis-related protease P69B of tomato. *Plant Physiol* **138**, 1785-1793
832 (2005).
833 48 Paulus, J. K. *et al.* Extracellular proteolytic cascade in tomato activates immune
834 protease Rcr3. *Proc Natl Acad Sci U S A* **117**, 17409-17417 (2020).
835 49 Stührwohldt, N., Bühler, E., Sauter, M. & Schaller, A. Phytosulfokine (PSK)
836 precursor processing by subtilase SBT3.8 and PSK signaling improve drought
837 stress tolerance in Arabidopsis. *J Exp Bot* **72**, 3427-3440 (2021).

50 Stegmann, M. *et al.* RGI-GOLVEN signaling promotes cell surface immune receptor abundance to regulate plant immunity. *EMBO Reports* **23**, e53281 (2022).

51 Zhang, H. *et al.* A Plant Phytosulfokine Peptide Initiates Auxin-Dependent Immunity through Cytosolic Ca(2+) Signaling in Tomato. *Plant Cell* **30**, 652-667 (2018).

52 Igarashi, D., Tsuda, K. & Katagiri, F. The peptide growth factor, phytosulfokine, attenuates pattern-triggered immunity. *Plant J* **71**, 194-204 (2012).

53 Kumar, S., Stecher, G., Li, M., Knyaz, C. & Tamura, K. MEGA X: molecular evolutionary genetics analysis across computing platforms. *Mol Biol Evol* **35**, 1547-1549 (2018).

54 Ranf, S. *et al.* Microbe-associated molecular pattern-induced calcium signaling requires the receptor-like cytoplasmic kinases, PBL1 and BIK1. *BMC Plant Biol* **14**, 374 (2014).

55 Lampropoulos, A. *et al.* GreenGate---a novel, versatile, and efficient cloning system for plant transgenesis. *PloS One* **8**, e83043 (2013).

56 Gleave, A. P. A versatile binary vector system with a T-DNA organisational structure conducive to efficient integration of cloned DNA into the plant genome. *Plant Mol Biol* **20**, 1203-1207 (1992).

57 Castel, B., Tomlinson, L., Locci, F., Yang, Y. & Jones, J. D. G. Optimization of T-DNA architecture for Cas9-mediated mutagenesis in Arabidopsis. *PloS One* **14**, e0204778 (2019).

58 Colaianni, N. R. *et al.* A complex immune response to flagellin epitope variation in commensal communities. *Cell Host Microbe* **29**, 635-649 (2021).

59 Frickey, T. & Lupas, A. CLANS: a Java application for visualizing protein families based on pairwise similarity. *Bioinformatics* **20**, 3702-3704 (2004).

60 Kesten, C. *et al.* Pathogen-induced pH changes regulate the growth-defense balance in plants. *EMBO J* **38**, e101822 (2019).

61 Huerta, A. I., Kesten, C., Menna, A. L., Sancho-Andrés, G. & Sanchez-Rodriguez, C. In-plate quantitative characterization of Arabidopsis thaliana susceptibility to the fungal vascular pathogen fusarium oxysporum. *Curr Protoc Plant Biol* **5**, e20113 (2020).

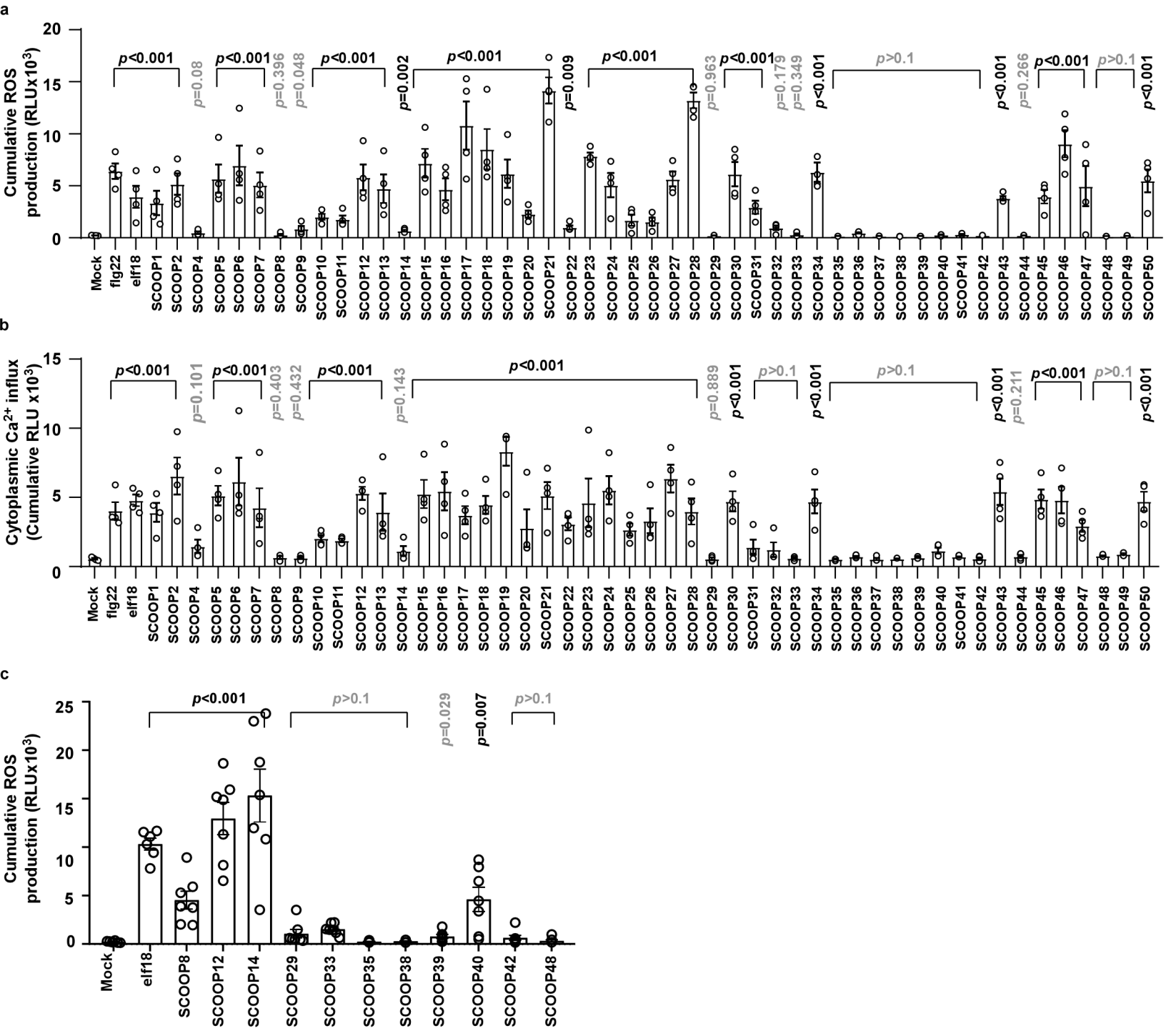
a
Cumulative ROS production (RLUx10³)
b
Cytoplasmic Ca²⁺ influx (Cumulative RLU x10³)
c
Cumulative ROS production (RLUx10³)
Mock
flg22
elf18
SCOOP1
SCOOP2
SCOOP4
SCOOP5
SCOOP6
SCOOP7
SCOOP8
SCOOP9
SCOOP10
SCOOP11
SCOOP12
SCOOP13
SCOOP14
SCOOP15
SCOOP16
SCOOP17
SCOOP18
SCOOP19
SCOOP20
SCOOP21
SCOOP22
SCOOP23
SCOOP24
SCOOP25
SCOOP26
SCOOP27
SCOOP28
SCOOP29
SCOOP30
SCOOP31
SCOOP32
SCOOP33
SCOOP34
SCOOP35
SCOOP36
SCOOP37
SCOOP38
SCOOP39
SCOOP40
SCOOP41
SCOOP42
SCOOP43
SCOOP44
SCOOP45
SCOOP46
SCOOP47
SCOOP48
SCOOP49
SCOOP50
p<0.001
p=0.08
p<0.001
p=0.396
p=0.048
p<0.001
p=0.002
p<0.001
p=0.009
p<0.001
p=0.963
p<0.001
p=0.179
p=0.349
p<0.001
p>0.1
p<0.001
p=0.266
p<0.001
p>0.1
p<0.001
p=0.101
p<0.001
p=0.403
p=0.432
p<0.001
p=0.143
p<0.001
p=0.889
p<0.001
p>0.1
p<0.001
p>0.1
p<0.001
p=0.211
p<0.001
p>0.1
p<0.001
p>0.1
p=0.029
p=0.007

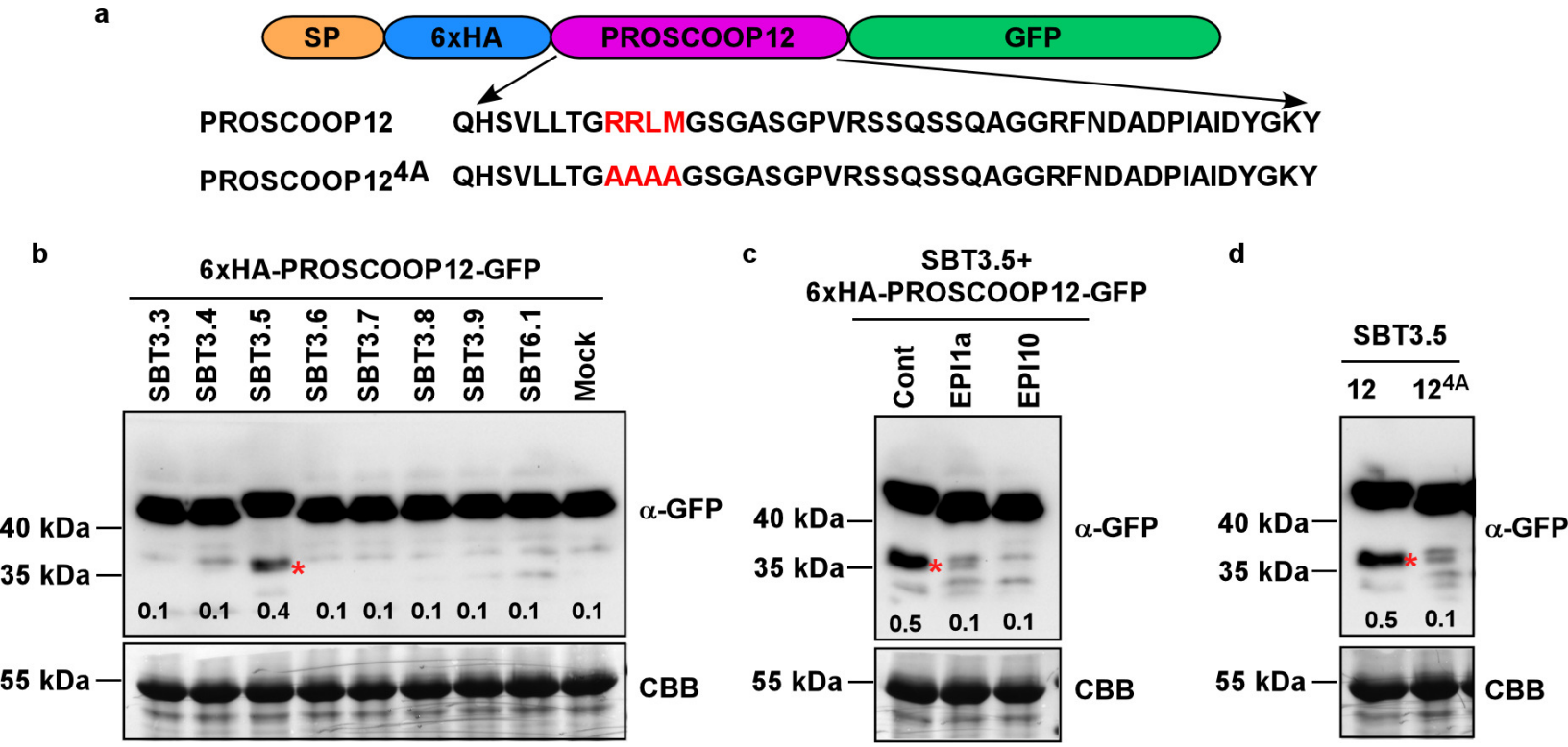
a
SP
6xHA
PROSCOOP12
GFP
PROSCOOP12 QHSVLLTGRRLMGSGASGPVRSSQSSQAGGRFNDADPIAIDYGKY
PROSCOOP12^4A QHSVLLTGAAAAGSGASGPVRSSQSSQAGGRFNDADPIAIDYGKY
b
6xHA-PROSCOOP12-GFP
SBT3.3
SBT3.4
SBT3.5
SBT3.6
SBT3.7
SBT3.8
SBT3.9
SBT6.1
Mock
40 kDa
35 kDa
55 kDa
α-GFP
CBB
0.1 0.1 0.4 0.1 0.1 0.1 0.1 0.1 0.1
c
SBT3.5+
6xHA-PROSCOOP12-GFP
Cont
EPI1a
EPI10
40 kDa
35 kDa
55 kDa
α-GFP
CBB
0.5 0.1 0.1
d
SBT3.5
12
12^4A
40 kDa
35 kDa
55 kDa
α-GFP
CBB
0.5 0.1

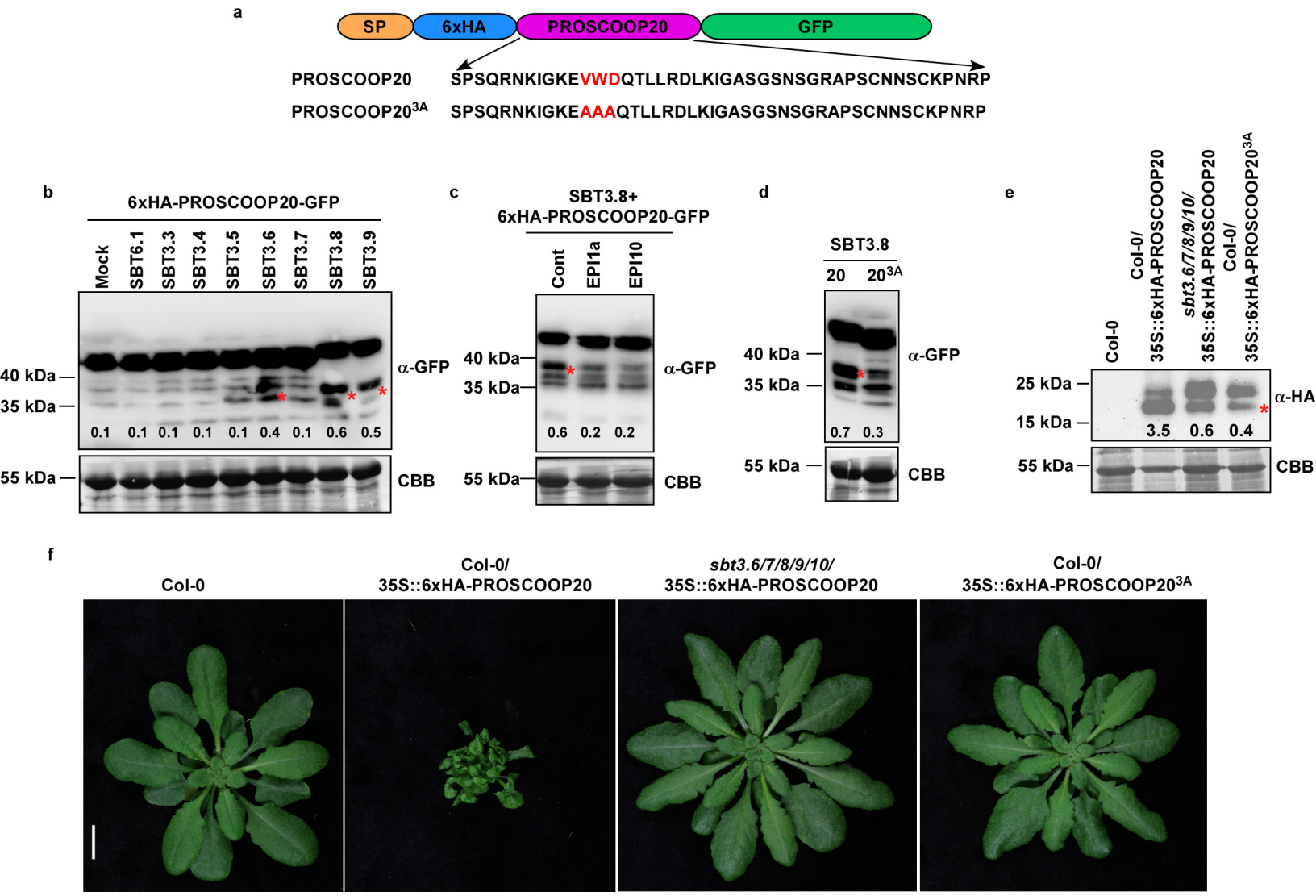
a
SP
6xHA
PROSCOOP20
GFP
PROSCOOP20 SPSQRNKIGKEVWDQTLLRDLKIGASGSNSGRAPSCNNSCKPNRP
PROSCOOP20^3A SPSQRNKIGKEAAAQTLLRDLKIGASGSNSGRAPSCNNSCKPNRP
b
6xHA-PROSCOOP20-GFP
Mock
SBT6.1
SBT3.3
SBT3.4
SBT3.5
SBT3.6
SBT3.7
SBT3.8
SBT3.9
40 kDa
35 kDa
0.1 0.1 0.1 0.1 0.1 0.4 0.1 0.6 0.5
α-GFP
55 kDa
CBB
c
SBT3.8+
6xHA-PROSCOOP20-GFP
Cont
EPI1a
EPI10
40 kDa
35 kDa
0.6 0.2 0.2
α-GFP
55 kDa
CBB
d
SBT3.8
20
20^3A
40 kDa
35 kDa
0.7 0.3
α-GFP
55 kDa
CBB
e
Col-0
Col-0/ 35S::6xHA-PROSCOOP20
sbt3.6/7/8/9/10/ 35S::6xHA-PROSCOOP20
Col-0/ 35S::6xHA-PROSCOOP20^3A
25 kDa
15 kDa
3.5 0.6 0.4
α-HA
55 kDa
CBB
f
Col-0
Col-0/ 35S::6xHA-PROSCOOP20
sbt3.6/7/8/9/10/ 35S::6xHA-PROSCOOP20
Col-0/ 35S::6xHA-PROSCOOP20^3A

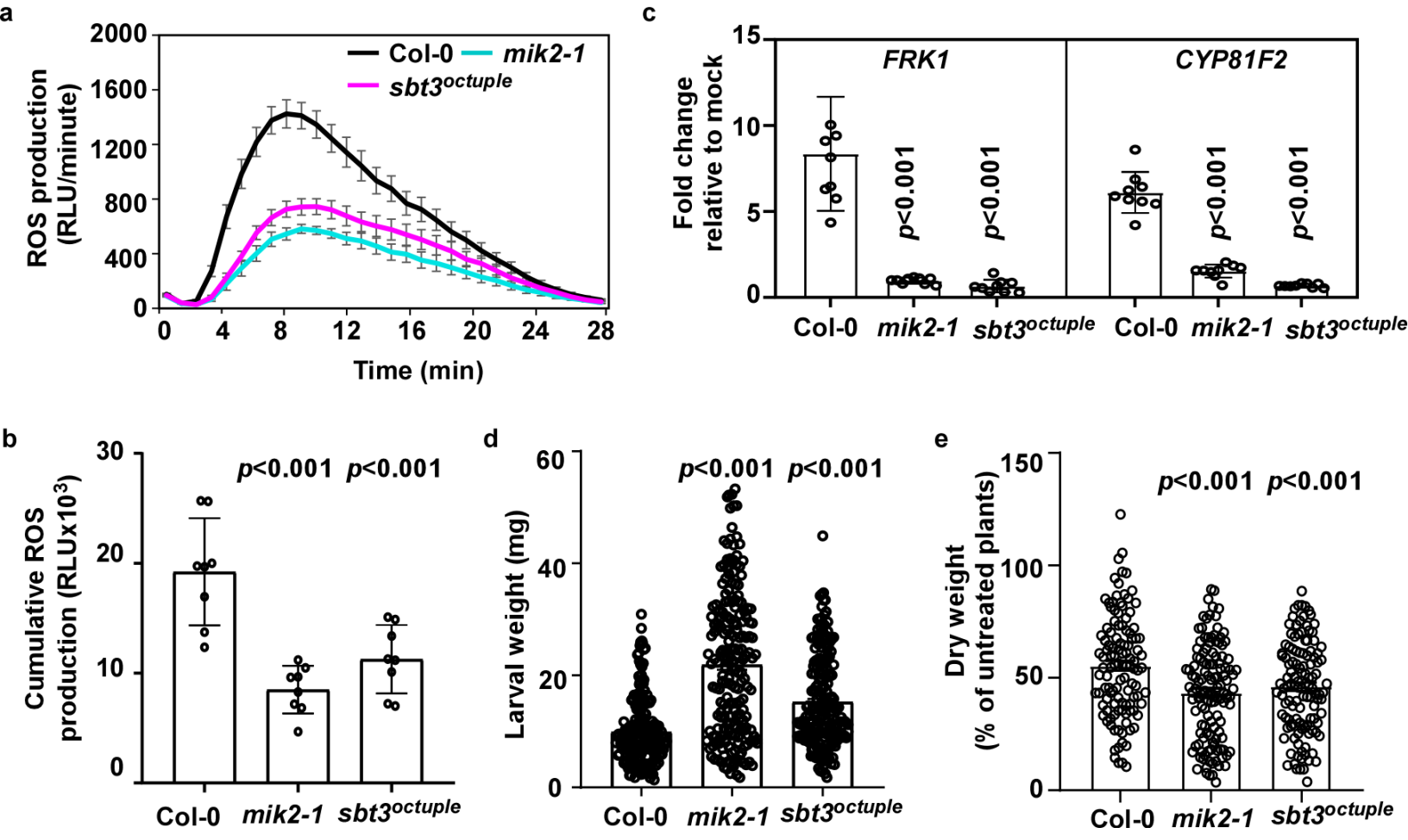
a
ROS production (RLU/minute)
2000
1600
1200
800
400
0
Col-0
mik2-1
sbt3octuple
0
4
8
12
16
20
24
28
Time (min)
c
Fold change relative to mock
15
10
5
0
FRK1
CYP81F2
p<0.001
p<0.001
p<0.001
p<0.001
Col-0
mik2-1
sbt3octuple
Col-0
mik2-1
sbt3octuple
b
Cumulative ROS production (RLUx10³)
30
20
10
0
p<0.001
p<0.001
Col-0
mik2-1
sbt3octuple
d
Larval weight (mg)
60
40
20
0
p<0.001
p<0.001
Col-0
mik2-1
sbt3octuple
e
Dry weight (% of untreated plants)
150
100
50
0
p<0.001
p<0.001
Col-0
mik2-1
sbt3octuple